SHORT NOTES ON ALASKAN GEOLOGY - 1977

GEOLOGIC REPORT 55

Recent research on Alaskan geology

STATE OF ALASKA

Jay S. Hammond, *Governor*

Robert E. LeResche, *Commissioner, Dept. of Natural Resources*

Ross G. Schaff, *State Geologist*

'Short Note' Editorial Policy

This document comprises short contributions on recent investigations of a limited scope on Alaskan geology. Manuscripts are accepted for review with certain qualifications: That manuscripts must not have been published or submitted for publication elsewhere; that all persons listed as authors have given their approval for submission of the paper; and that any person cited as a source of personal communication has approved such a citation.

Two copies of the manuscript, typed double spaced including references and figure captions, should be submitted to Editor, Alaska Division of Geological & Geophysical Surveys, Box 80007, College, AK 99708. No more than seven double-spaced manuscript pages (2000 words), including references, figures, and tables, will be accepted. All figures should be camera ready and suitable for black-and-white reproduction at a maximum size of 6-1/2 by 9-1/2 inches—foldout or color art will not be accepted. Contributors should keep one copy of material submitted. All manuscripts will be reviewed by the Alaska DGGS publications committee.

Deadline for manuscripts for the next *Short Notes on Alaskan Geology* is April 15, 1978.

Cover photo: Aerial view of Katmai caldera, looking north-northeast. North glacier and remnant of Katmai peak in left background. Note darkened zone of upwelling near center of lake. Photo courtesy of Austin Post, U.S. Geological Survey, Aug. 26, 1969.

For sale by Alaska Division of Geological and Geophysical Surveys, P.O. Box 80007, College, 99708; 3327 Fairbanks St., Anchorage, 99503; P.O. Box 2438, Ketchikan, 99901; and Pouch M, Juneau, 99811.

CONTENTS

A GIVETIAN (LATE MIDDLE DEVONIAN) FAUNA FROM HEALY B-4 QUADRANGLE, CENTRAL ALASKA RANGE, ALASKA

By Robert B. Blodgett[1]

GENERAL STATEMENT

Moffit (1915) reported an occurrence of poorly preserved fossils from a limestone body on the Jack River near Cantwell, Alaska. The limestone body was reported to occur between 'walls' of slate and conglomerate. The fossils were identified by Edwin Kirk, who indicated that they were either late Middle Devonian (Givetian) or early Late Devonian (Frasnian) in age. This locality was re-collected by the author during the summers of 1974 and 1976 as part of a continuing study of Devonian invertebrate fossils of interior Alaska. The limestone consists of dark-gray micrite cut by many veins of recrystallized white calcite. In most places the limestone has been thoroughly recrystallized and altered so as to obscure the nature of the fossils. However, one small pod within the massive limestone was found to yield poorly preserved but generically identifiable fossils. The rocks of the area have been folded and weakly metamorphosed; no formal stratigraphic names have been applied to them.

PALEONTOLOGY

The following taxa have been identified:

- Coelenterata
  - *Cladopora* sp.
  - *Dendrostella* sp.
  - auloporoid tabulate corals
  - lamellar stromatoporoids
- Brachiopoda
  - *Leiorhynchus* spp.
  - *Emanuella* sp.
  - *Ladjia* sp.
- Arthopoda (Cl. Trilobita)
  - *Dechenella (Dechenella)* sp.
- Indeterminate gastropods

The rugose coral genus *Dendrostella* is found primarily in rocks of Givetian age, but has been reported from the late Eifelian of the USSR (Pedder, 1964). *Dendrostella* is a common element in Alaskan faunas of Givetian age and has been reported from the Tolovana Limestone of the Livengood quadrangle, from an unnamed stratigraphic unit in the southeastern part of the Sleetmute quadrangle, and from the Skajit(?) Limestone of the western Brooks Range (Oliver and others, 1975). The rhynchonelloid brachiopod *Leiorhynchus* is a cosmopolitan genus that ranges from late-early Middle Devonian (late Eifelian) to middle-early Late Devonian (middle Frasnian) time in western Canada (McLaren, 1962). The ambocoeliid brachiopod *Emanuella* is known from Middle and Upper Devonian strata and is cosmopolitan. *Ladjia*, also an ambocoelliid, is known from the Frasnian of Australia and from Givetian-Frasnian boundary beds of western North America (Pedder, 1975). The trilobite *Dechenella (Dechenella)* ranges throughout the entire Middle Devonian (Eifelian-Givetian) and is a common faunal element in rocks of this age from western North America and the Canadian Arctic Islands (Ormiston, 1967).

This faunal assemblage strongly indicates that the limestone body is referable to the Givetian Stage.

FOSSIL LOCALITY

The fossils were found near a prominent overhanging limestone cliff exposed along the north side of the Denali Highway approximately 1.3 mile east of its junction with the Anchorage-Fairbanks Highway, east-center sec. 3, T. 18 S., R. 7 W., Healy B-4 quadrangle, lat 63°23'00"N., long 148°41'46"W. (University of Alaska Museum paleontology locality A-713).

ACKNOWLEDGMENTS

I would like to thank Drs. Richard C. and Carol W. Allison of the University of Alaska for their critical review of the manuscript. This research was supported in part by the Geist Fund of the University of Alaska Museum.

REFERENCES CITED

McLaren, D.J., 1962, Middle and early Upper Devonian rhynchonelloid brachiopods from western Canada: Geol. Surv. Canada Bull. 86, 122 p.

Moffit, F.H., 1915, The Broad Pass Region, Alaska: U.S. Geol. Survey Bull. 608, 80 p.

Oliver, W.A., Jr., Merriam, C.W., and Churkin, Michael, Jr., 1975, Ordovician, Silurian, and Devonian corals of Alaska: U.S. Geol. Survey Prof. Paper 823-A, p. 13-44.

Ormiston, A.R., 1967, Lower and Middle Devonian trilobites of the Canadian Arctic Islands: Geol. Survey Canada Bull. 153, 148 p.

Pedder, A.E.H., 1964, Correlation of the Canadian Middle Hume and Nahanni Formations by tetracorals: Paleontology, v. 7, p. 430-451.

______, 1975, Revised megafossil zonation of Middle

[1]Division of Geosciences, University of Alaska, Fairbanks, AK 99701.

and lowest Upper Devonian strata, central Mackenzie Valley: Geol. Survey Canada Paper 75-1, pt. A, p. 571-576.

PROBABLE KARST TOPOGRAPHY NEAR JADE MOUNTAINS, SOUTHWESTERN BROOKS RANGE, ALASKA

By G.H. Pessel[1]

A number of small depressions are located in the glacially sculptured foothills north of the eastern end of the Jade Mountains, in the Ambler River quadrangle of northern interior Alaska. The depressions appear to be sinkholes or collapse features in carbonate rock and are probably indicative of karst topography, a geomorphic landform not previously observed in the permafrost regime of northern Alaska.

R.E. Garland (DGGS) and I.L. Tailleur (USGS) noted the depressions as anomalous features in the foothills of the Jade Mountains during a geologic mapping project in 1972. Garland and Pessel investigated two of the depressions later in the course of the mapping project. J.M. Zdepski (DGGS), W.P. Brosge' (USGS), and Tailleur inspected the area from the air in 1973, and found indications of underground drainage in some stream channels off the north slope of the western Jade Mountains. Although no conclusive evidence for the origin of the depressions could be found, the most likely explanation appears to be some form of karst topography in the classic sense, rather than the thermokarst degradation so common in northern Alaska surficial deposits.

The sinkholes are roughly conical, 30-45 m across and about 15 m deep (figs. 1-3). They do not connect to surface drainage, and show no evidence of water filling during spring breakup or periods of heavy rain.

The low foothills in the area of the sinkholes are clearly the result of glacial erosion. Cirque basins indent the northern crest of the Jade Mountains, and merge with smooth, trough-shaped valleys. Some of the valleys are cut by sharply incised modern stream channels in their lower reaches. Glacial drift covers most of the foothills, and glacial erratics are common. Low vegetation, typical of the southern foothills of the southern Brooks Range, covers most of the area, and open slopes are covered with grass tussocks, typical of the Arctic permafrost regime. Scattered outcrops are found throughout the area, and include rubble-covered hills and some cutbanks in the modern stream courses.

Vegetation and a thin mantle of surficial deposits mask the bedrock throughout most of the foothills. Geologic maps of the area have been published at a scale of 1:250,000 (Patton, Miller, and Tailleur, 1968; Pessel and Brosge', 1977). Figure 4 is an outcrop map at a scale of 1:63,360 of the area where most of the depressions are located. The mass of the Jade Mountains consists largely of shallow-seated mafic igneous rocks and ultramafics, including serpentinite and dunite, which form an ophiolite-like sequence that flanks the southern edge of the Brooks Range. In the foothills north of the Jade Mountains, the bedrock appears to consist mainly of dark phyllites, light-gray carbonates, and dark-gray cherty carbonates, all of probable Paleozoic age. A few scattered outcrops of mafic igneous rocks also occur in the foothills. Outcrops in stream cutbanks and rubble-covered slopes indicate that the most likely bedrock in the area of the sinkholes is the carbonates. Blocks of dark cherty limestone and a possible outcrop of the same type of rock were found

[1]Alaska Division of Geological and Geophysical Surveys, Anchorage, AK 99501.

Figure 1. Aerial view of depression, looking southwest.

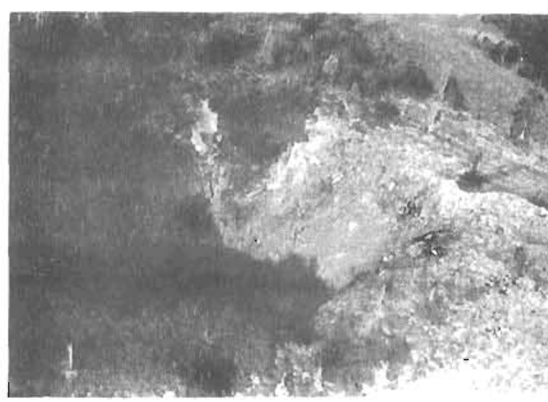

Figure 2. Closer view of same sinkhole.

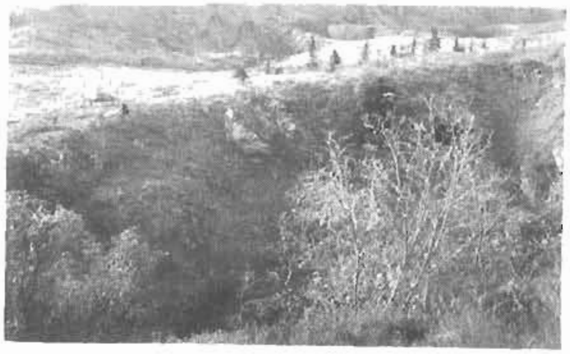

Figure 3. Another depression in northern Jade Hills. Slope not as steep as sinkhole in figs. 1 and 2.

on the side and floor of one of the sinkholes.

Caverns and internal drainage channels in the carbonates are a likely possibility. One of the nearby streams disappears into its bed during low water and reappears about a mile or so downstream. In the Cosmos Hills, to the east, the shaft at the Bornite mine was flooded by water entering the workings in carbonate rocks that are correlative with those in the Jade Mountains. Elsewhere in the Brooks Range, springs are common in similar carbonate rocks, indicating the presence of well-developed subterranean channels.

The age of formation of caverns and channels in the carbonates, if such is indeed the correct explanation for the sinkholes, is not clear. The formation of solution channels within the carbonates would logically be controlled, to some extent, by the presence of permafrost and the climatic history of the area. The depressions are not filled with glacial drift, possibly indicating that they were formed after the last ice age.

References

Patton, W.W., Jr., Miller, T.P., and Tailleur, I.L., 1968, Regional geologic map of the Shungnak and southern part of the Ambler River quadrangles, Alaska: U.S. Geol. Survey Misc. Geol. Inv. Map I-554.

Pessel, G.H., and Brosge', W.P., 1977, Preliminary reconnaissance geologic map of the Ambler River quadrangle, Alaska: U.S. Geol. Survey open-file rept. 77-28.

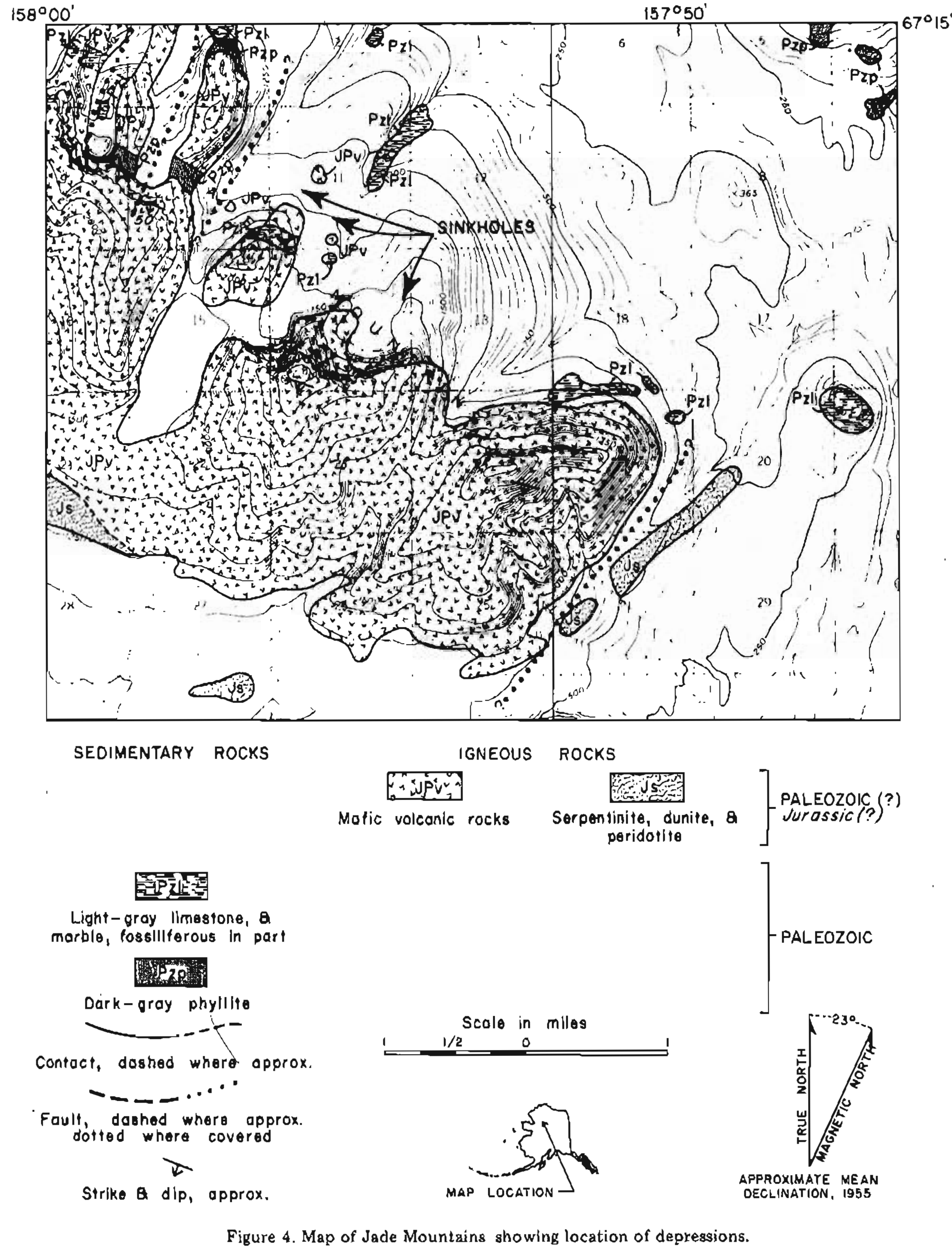

Figure 4. Map of Jade Mountains showing location of depressions.

TECTONIC SIGNIFICANCE OF THE KNIK RIVER SCHIST TERRANE, SOUTH-CENTRAL ALASKA

By J.R. Carden[1] and J.E. Decker[2]

In a reconnaissance study of the bedrock geology of the Chugach Mountains near Anchorage, Alaska, Clark (1972a) distinguished a group of undifferentiated metamorphic rocks extending from near Eagle River to the Knik River. A recent map by Magoon and others (1976) extends this terrane northeast along strike to the area of Coal Creek (fig. 1). This investigation is a preliminary interpretation of the tectonic significance of these metamorphic rocks, which we here informally call the Knik River schist terrane.

Near Eklutna the Knik River schist terrane is composed of marble, siliceous argillite, metachert, metasandstone, and metavolcanic rocks (Clark, 1972a). The marble forms discontinuous podlike layers and lenses that can be seen from the highway. The dominant metavolcanic unit is an actinolite schist that forms massive steep-sided outcrops near the Knik River. Rocks from the schist terrane have been metamorphosed to greenschist and possibly low-grade amphibolite facies. Most outcrops are highly sheared and display melangelike characteristics.

We suggest that the Knik River schist terrane represents a segment of the Early Jurassic subduction complex that extends discontinuously from the Kodiak Islands to the Canadian border and possibly into southeastern Alaska (Forbes and others, 1976, 1977). Carden and others (1977) have described the schists of this complex in the areas of the Kodiak Islands and Seldovia-Port Graham, near the western end of the Kenai Peninsula. The complex there consists of a series of volcanic and deep-sea lithologies that have been metamorphosed to the blueschist-greenschist-facies boundary. The age determined from this schist terrane indicates emplacement of the complex by Early Jurassic time. This timing is consistent with the biostratigraphy of associated forearc basin deposits (Burk, 1965; Detterman and Hartsock, 1966) and K-Ar ages of Jurassic rocks from the associated Alaska-Aleutian Range plutonic arc (Reed and Lanphere, 1973).

We believe the Knik River schist terrane represents an extension of the Seldovia-Kodiak Islands schist terrane because both occupy the same tectonic position relative to major geologic features on the southern Alaska margin. They are immediately tectonically above the Border Ranges Fault (MacKevett and Plafker, 1974), a suture zone that represents a major Mesozoic plate boundary separating older schists of the upper plate from volcanogenic sedimentary rocks of the McHugh-Uyak and Valdez Complexes of the lower plate (MacKevett and Plafker, 1974). These rocks represent a later pulse of subduction in Cretaceous time (Moore and Connelly, 1976). In the Kodiak and Seldovia area, slivers of a dismembered ophiolite occur between the schists and the Border Ranges Fault (Carden and others, 1977). The same ultramafic rocks are represented in the Anchorage area by the mafic-ultramafic rocks of the Wolverine Complex (Clark, 1972b), which occur between the Knik River schist terrane and the McHugh Complex. The Kodiak-Seldovia and Knik River schist belts are both bound on the northwest by Mesozoic shelf rocks that are interpreted by Moore (1974) as a forearc sequence. Rocks of both terranes are structurally similar and are characterized by melangelike deformation and an isoclinal overturned fold style.

A single K-Ar age of 173 $\pm$ 7 m.y. obtained on an actinolite separate from an actinolite-epidote schist greenschist collected at the mouth of the Knik River in the Anchorage B-6 quadrangle (fig. 1, table 1) is the first radiometric age reported from the complex. Although the apparent age is Lower Jurassic, it is significantly younger than the average of nine K-Ar ages determined for actinolites and white micas (189 $\pm$ 3 m.y.) from the schist of the Seldovia-Kodiak Islands terrane (Carden and others, 1977). This difference may be due to thermal overprinting by a pluton, dated at 161 $\pm$ 5 m.y. (Clark, 1972a), 2 km from the sampled schist outcrop (fig. 1). Agreement at the 67 percent confidence level between the pluton and the schist date suggests that the actinolite schist age may have been either totally or partially reset from an older value.

An alternative hypothesis is that the Knik River schists may have had a different time on uplift than did the Seldovia-Kodiak schists. Rapid tectonic emergence is necessary to preserve blueschist facies mineral assemblages formed at depth (Ernst, 1971). If uplift is not sufficiently rapid, blueschist mineral assemblages will be thermally upgraded to at least the greenschist facies. Furthermore, the slower rate of tectonic emergence will produce younger apparent ages because minerals will pass through their characteristic argon-blocking isotherms at a later time. There have been no blueschist assemblages yet reported from the Knik River schist terrane and preliminary evidence suggests that these rocks have undergone greenschist-blueschist-facies metamorphism.

[1]Geophysical Institute, University of Alaska, Fairbanks, AK 99701.
[2]Dept. of Geology, Stanford University, Stanford, CA 94305.

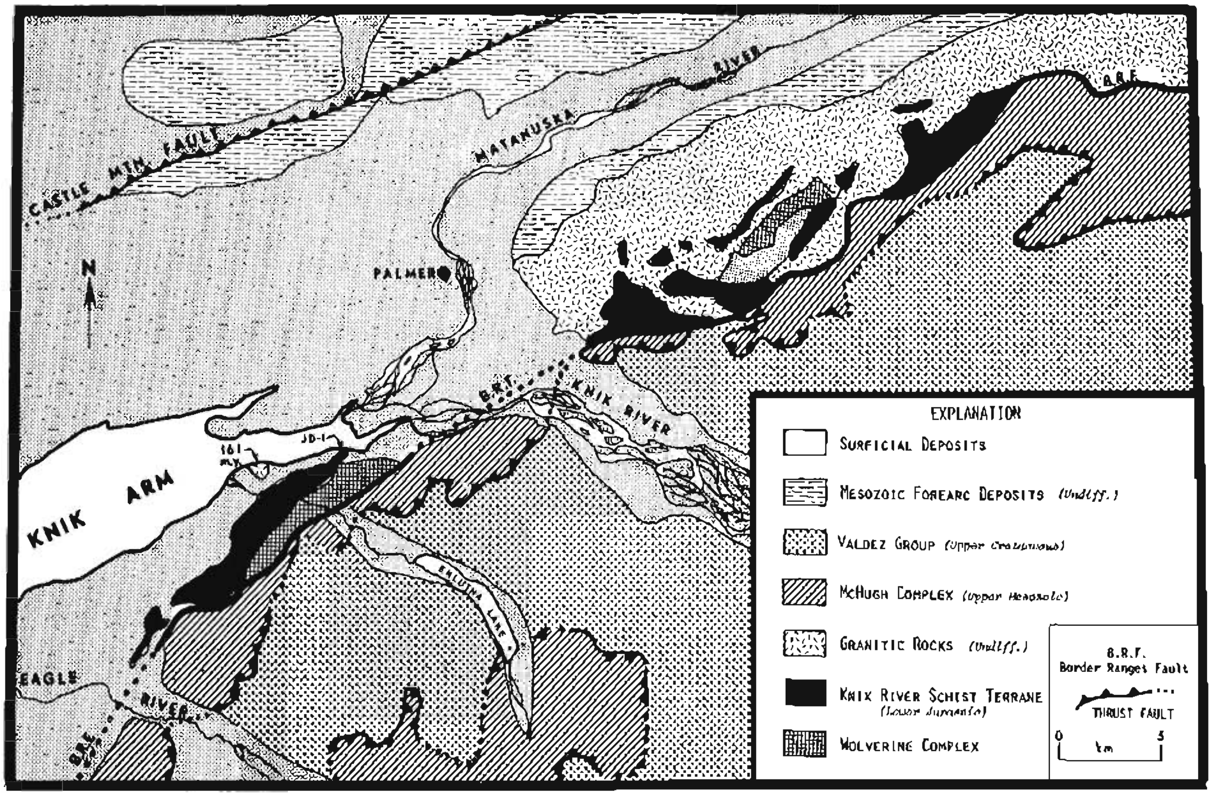

Figure 1. Generalized geologic map showing the location of the proposed Knik River schist terrane in relation to other major tectonic units in the area (after Magoon and others, 1976). Sample JD-1 and location of 161-m.y. pluton are given.

Table 1. *K-Ar analytical data.*[1, 2]

Sample	Rock type	Mineral dated	K_2O (wt.%)	Sample weight (g)	$^{40}Ar_{rad}$ (moles/g) x 10^{-11}	$\frac{^{40}Ar_{rad}}{^{40}K}$ x 10^{-3}	$\frac{^{40}Ar_{rad}}{^{40}Ar\ total}$	Age $\pm 1\sigma$ (m.y.)
JD-1 (76181)	Greenschist	Actinolite	0.165 0.165 0.175 0.164 $\bar{x}$=0.167	1.3690	4.489	10.63	0.644	173±7

[1] Analytical techniques have been described previously by Turner and others (1973).
[2] Constants used: λ_ϵ = 0.585 x 10^{-10}/yr, λ_β = 4.72 x 10^{-10}/yr, $^{40}K/K_{tot}$ = 1.19 x 10^{-4} mol/mol

Because we cannot support one age interpretation over another from the limited data presently available, the Knik River schist terrane merits further study. Detailed mapping and additional dating are needed for a clear understanding of the age and mode of emplacement of these rocks in relation to other metamorphic terranes to the northeast.

ACKNOWLEDGMENTS

W.G. Gilbert and D.L. Turner critically reviewed this manuscript and offered many helpful suggestions. We wish to thank Diane Duvall for mineral separations and K-Ar determinations and Susan Karl for field assistance.

REFERENCES CITED

Burk, C.A., 1965, Geology of the Alaska Peninsula Island arc and continental margin: Geol. Soc. America Mem. 99. 250 p.

Carden, J.R., Connelly, Wm., Forbes, R.B., and Turner, D.L., 1977, Blueschists of the Kodiak Islands, Alaska: An extension of the Seldovia schist terrane: Geology (in press).

Clark, S.H.B., 1972a, Reconnaissance bedrock geologic map of the Chugach Mountains near Anchorage, Alaska: U.S. Geol. Survey Mineral Inv. Field Studies Map MF-350, 1:250,000.

_____ , 1972b, The Wolverine Complex, a newly discovered layered ultramafic body in the western Chugach Mountains, Alaska: U.S. Geol. Survey Open-File Rept. 72-70 (522), 9 p.

Detterman, R.L., and Hartsock, J.K., 1966, Geology of the Iniskin-Tuxedni region, Alaska: U.S. Geol. Survey Prof. Paper 512, 78 p.

Ernst, W.G., 1971, Metamorphic zonation on presumably subducted lithospheric plates from Japan, California, and the Alps: Contr. Mineralogy and Petrology, v. 34, p. 43-59.

Forbes, R.B., Carden, J.R., and Connelly, Wm., 1976, The Kodiak-Chugach-Chichagof terranes - A newly defined Alaskan blueschist belt: Am. Geophys. Union abstract (EOS), v. 57, p. 351.

Forbes, R.B., Carden, J.R., Turner, D.L., and Connelly, Wm., 1977, Tectonic implications of Alaskan blueschist terranes: Program and Abstracts, 1977 Alaska Geol. Soc. Symposium, Anchorage, Alaska, p. 21-22.

MacKevett, E.M., and Plafker, George, 1974, The Border Ranges Fault in south-central Alaska: U.S. Geol. Survey Jour. Res., v. 2, p. 323-329.

Magoon, L.B., Adkinson, W.L., and Egbert, R.M., 1976, Map showing geology, wildcat wells, Tertiary plant fossil localities, K-Ar age dates, and petroleum operations, Cook Inlet area, Alaska: U.S. Geol. Survey Misc. Geol. Inv. Map I-1019.

Moore, J.C., 1974, The ancient continental margins of Alaska, *in* The Geology of continental margins (C. Burk and C. Drake, eds): New York, Springer-Verlag, p. 811-815.

Reed, B.L., and Lanphere, M.A., 1973, Alaska-Aleutian Range batholith - Geochronology, chemistry, and relation to circum-Pacific plutonism: Geol. Soc. America Bull., v. 84, p. 2583-2610.

Turner, D.L., Forbes, R.B., and Naeser, C.W., 1973, Radiometric ages of Kodiak Seamount and Giacomini Guyot, Gulf of Alaska: Implications for circum-Pacific tectonics: Science, v. 182, p. 579-581.

GEOCHRONOLOGY OF SOUTHERN PRINCE OF WALES ISLAND, ALASKA

By Donald L. Turner,[1] Gordon Herreid,[2] and Thomas K. Bundtzen[2]

INTRODUCTION

This paper summarizes the results of a radiometric dating reconnaissance of the southern part of Prince of Wales Island. A more comprehensive summary of the geology and mineral deposits of this area will be given in a future paper (Herreid and others, in press).

Twenty total-fusion ^{40}K-^{40}Ar mineral and whole-rock ages were determined for 14 igneous and metamorphic rocks from the Craig A-2 quadrangle and vicinity (fig. 1). Analytical work was done in the Geochronology Laboratory of the Geophysical Institute, University of Alaska, Fairbanks. Analytical techniques used have been described previously (Turner and others, 1973). Analytical data for age determinations are given in table 1 (p. 16). Sample locations are shown in figure 2, a generalized geologic map modified from Herreid and others (in press).

WALES GROUP

Earlier workers mapped the regional metamorphic basement rocks on Prince of Wales Island as the "Wales Series" or Wales Group (Brooks, 1902; Buddington and Chapin, 1929). In this paper, the more strongly metamorphosed rocks are considered to be Wales Group, following the usage of Herreid and others (in press). They contrast with the less metamorphosed Middle Ordovician Descon Formation and with Devonian and younger bedded rocks nearby. All the Wales Group rocks in the Craig A-2 quadrangle appear to have had a similar metamorphic history, but could include rocks of different premetamorphic ages. Lithologies include varying amounts of marble, tuffaceous schist, phyllite, metavolcanics, quartz sericite schist, and migmatitic gneiss. These rocks have undergone greenschist-facies metamorphism (Herreid and others, in press).

Near Eek Point, Wales Group greenschists contain broken and rotated relict crystals of hornblende in a matrix of chlorite, albite, and tremolite. The hornblende shows incipient overgrowths of tremolite. These textural relationships and the presence of interbedded metakeratophyres indicate that these greenschists represent original volcanic ash layers in the Wales Group and that the hornblende represents a primary volcanic mineral that was partially altered to tremolite during greenschist-facies metamorphism.

Minerals and whole-rock samples ranging from 0.445 to 0.034 percent K_2O were dated. The ages of the three minerals (hornblendes) with the highest potassium contents (0.285 to 0.445 percent K_2O) agree within analytical uncertainty and have a mean value of 486 ± 15 m.y. (table 1). Two hornblendes (DT72-51A and -52C) are from greenschists near Eek Point, with tremolite overgrowths as discussed above. The third hornblende dated (72C149 + 72C136) comes from a migmatite gneiss from Sunny Cove that appears to have undergone the same greenschist-facies metamorphism as the Wales Group (Herreid and others, in press).

Tremolites from the two greenschists (DT72-51A and -52C) and a whole-rock metakeratophyre (72C-174B) have very low potassium contents (0.034 to 0.053 percent) and yielded significantly higher apparent ages (661 to 526 m.y.). These results indicate that the tremolite and metakeratophyre ages are affected significantly by inherited argon—unlike the hornblendes, which have much higher potassium contents and therefore have produced larger quantities of radiogenic argon.

Although the tremolite and metakeratophyre apparent ages are discordant with the more reliable hornblende ages, all of these data collectively define a straight line (correlation coefficient 0.999) when plotted on a ^{40}Ar-^{40}K isochron diagram (fig. 3) and yield an isochron age of 475 m.y. The concordant hornblende ages and the fact that all of the age data fit an isochron suggest that the Wales Group was involved in a regional thermal event that cooled to argon-retention temperatures in Early Ordovician time.

The K-Ar data alone do not resolve the question of whether this Early Ordovician event represents the original greenschist-facies metamorphism of the Wales Group or a later thermal event that reset the K-Ar clock but did not reach high-enough temperatures to cause metamorphic recrystallization.

Churkin and Eberlein (1977), on the basis of preliminary U-Pb zircon data, report that metamorphic rocks of the Wales Group at Ruth Bay are intruded by an underformed and unmetamorphosed trondhjemite body that crystallized at least 730 m.y. ago. Assuming that this preliminary age will be confirmed by additional U-Pb work, they have proposed that greenschist-facies metamorphism of the Wales Group pre-

[1] Geophysical Institute and Solid-Earth Sciences Program, University of Alaska, Fairbanks, AK 99701.
[2] Alaska DGGS, College, AK 99708.

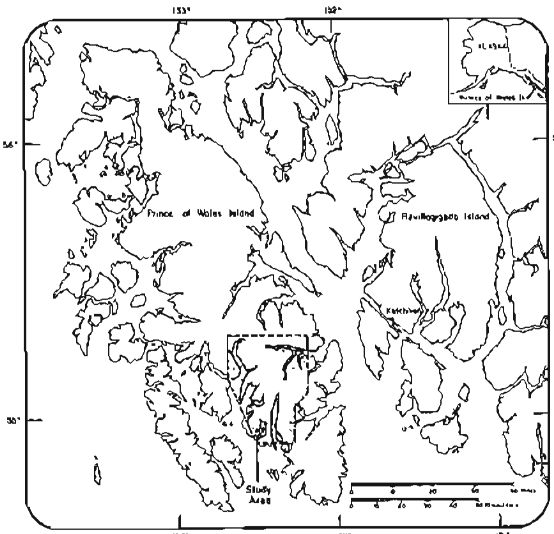

Figure 1. Location map of study area.

ceded the trondhjemite intrusion sometime during the Precambrian. If this age interpretation is correct, our K-Ar data indicate that a second thermal event affected these rocks after their Precambrian recrystallization. The zircon U-Pb ages were apparently unaffected by this thermal event, but the K-Ar system was reset to the Early Ordovician ages discussed above.

SILURIAN OR OLDER INTRUSIVE ROCKS

Hornblende from a deuterically altered granodiorite pluton on the north shore of Max Cove was dated at 421 ± 13 m.y. (DT72-58C). We consider this a minimum age because of the degree of alteration present. However, it agrees within analytical uncertainty with the hornblende K-Ar age of 446 ± 22 m.y. reported by Lanphere and others (1964) for a complex assemblage of granitic rocks ranging from diorite to quartz monzonite in the Bokan Mountain area, about 10 miles to the east. Lanphere has also determined hornblende K-Ar ages of 440 ± 13 and 432 ± 13 m.y. from a gabbroic body intruding rocks coeval with the Descon Formation on Sukkwan Island, about 10 miles south of Eek Point (G.D. Eberlein and M.A. Lanphere, pers. comm., 1977). These similar intrusive ages suggest that the 421-m.y. minimum age may be a reasonable estimate for the cooling age of the pluton at Max Cove. This pluton intrudes rocks of the Middle to Late Ordovician Descon Formation and is overlain by an Early to Middle Devonian basal conglomerate containing cobbles and boulders of deuterically altered granodiorite that is compositionally and texturally similar to the granodiorite of the pluton (Herreid and others, in press). These stratigraphic age constraints are in good agreement with the radiometric age evidence discussed above.

COPPER MOUNTAIN PLUTON AND RELATED INTRUSIVES

Seven samples of granodiorite and monzonite from the Copper Mountain pluton and related intrusive bodies yielded concordant hornblende ages averaging 102 ± 3 m.y. (table 1). Biotite from the granodiorite body at Hetta Lake, which appears to be a satellite of the Copper Mountain pluton, was dated at 105 ± 3 m.y., concordant with the 103 ± 3 m.y. age obtained from coexisting hornblende.

The concordant hornblende and biotite ages suggest argon-blocking isotherms for these two minerals passed through the granodiorite body in a time equal to or less than the analytical uncertainty of the age determinations. This suggestion of relatively rapid cooling is consistent with geologic evidence for shallow intrusion of these plutons discussed by Herreid and others (in press), and we therefore believe that the mid-Cretaceous age of 102 ± 3 m.y. represents the time of emplacement and cooling of the Copper Mountain pluton and its related intrusive bodies.

One of these bodies—a 1-mile-diameter granodiorite pluton at 2546 mountain, 3 miles east of the head of Nutkwa Inlet—cuts the Keete Inlet thrust. Its mean hornblende age of 102 m.y. establishes that regional thrusting occurred before mid-Cretaceous time.

CONTACT METAMORPHIC ROCKS

A zone of biotite hornfels crops out for a short distance along the west side of the south arm of Cholmondeley Sound. Biotite in the hornfelsed zone is discordant to foliation in the greenschist country rock of the Wales Group. This biotite was dated at 355 ± 11 m.y. (72C410). Although there is no exposed intrusive body in the area, the hornfelsed zone may be due to an unexposed intrusive body at depth. This hypothetical intrusive could be Devonian, assuming that the biotite age represents the age of intrusion.

A thrust sheet of actinolite hornfels caps the ridge northeast of Hetta Lake. Actinolite from this hornfels yields an apparent age of 216 ± 6 m.y. (DT72-60A). This age is interpreted as a partial resetting of older Wales Group rocks due to heating from the intrusion of the Copper Mountain pluton.

The hornfels aureole surrounding the Copper Mountain pluton was dated at Dell Island. Actinolite from hornfelsed Wales Group greenschist, about 1 mile from the contact of the pluton, gave an apparent age of 141 ± 4 m.y. (DT72-55A). This age probably represents nearly complete resetting of the Wales Group greenschist age by contact metamorphism.

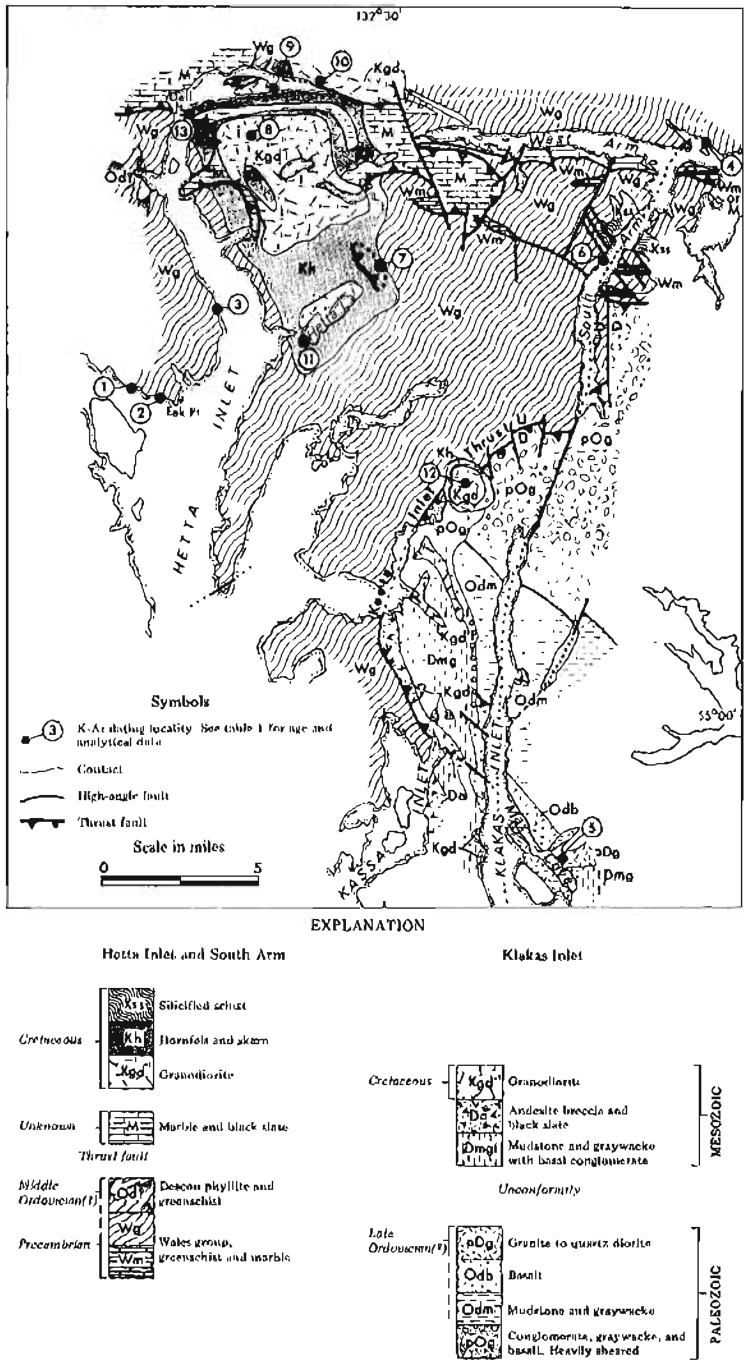

Figure 2. Geology of Craig A-2 quadrangle and vicinity, Prince of Wales Island, Alaska. Geology generalized from Herreid and others (in press).

Table 1. *Analytical data for ^{40}K-^{40}Ar age determinations*[1]

Map No.	Field No. (Lab. No.)	Rock type	Mineral dated	K_2O (Wt. %)	Sample weight (g)	$^{40}Ar_{rad.}$ (moles/g) $\times 10^{-11}$	$\frac{^{40}Ar_{rad.}}{^{40}K}$ $\times 10^{-3}$	$\frac{^{40}Ar_{rad.}}{^{40}Ar_{total}}$	Apparent age $\pm 1\sigma$ (m.y.)
				Wales Group					
1	DT72-51A (73078)	Greenschist	Tremolite	0.053,0.053, 0.052 $\bar{x}$=0.053	0.4524	5.534	41.60	0.698	*603±18[2]
1	DT72-51A (73095) Ar replicate	Greenschist	Tremolite	0.053,0.053, 0.052 $\bar{x}$=0.053	0.4536	5.724	43.03	0.591	*621±19 $\bar{x}$=*612
1	DT72-51A (73079)	Greenschist	Hornblende	0.349,0.346 0.343 $\bar{x}$=0.346	0.5103	26.97	30.86	0.855	465±14
1	DT72-51A (73096) Ar replicate	Greenschist	Hornblende	0.349,0.346, 0.343 $\bar{x}$=0.346	0.5116	28.99	33.17	0.861	496±15 $\bar{x}$=480
2	DT72-52C (73085)	Greenschist	Tremolite	0.044,0.045, 0.045 $\bar{x}$=0.045	0.6535	5.222	46.28	0.317	*661±20
2	DT72-52C (73094)	Greenschist	Hornblende	0.283,0.290, 0.282 $\bar{x}$=0.285	0.5583	23.25	32.30	0.622	484±14
3	72C174B (73031)	Metakeratophyre	Whole rock	0.035,0.034, 0.034 $\bar{x}$=0.034	1.1503	2.971	34.26	0.165	*510±15
3	72C174B (73033) Ar replicate	Metakeratophyre	Whole rock	0.035,0.034, 0.034 $\bar{x}$=0.034	1.0689	3.192	36.81	0.701	*543±16 $\bar{x}$=*526
4	72C149+ 72C136 (75085)	Migmatitic gneiss	Hornblende	0.440,0.450 x=0.445	0.9837	37.26	33.15	0.762	495±15
				Pluton at Max Cove					
5	DT72-58C (73100)	Altered granodiorite	Hornblende	0.570,0.580 $\bar{x}$=0.575	0.3551	40.12	27.62	0.938	421±13 (Minimum Age)

				Hornfels on Cholmondely Sound					
6	72C410 (73106)	Biotite hornfels	Biotite	8.127,8.140 $\bar{x}$=8.133	0.1937	469.8	22.87	0.960	355±11
				Actinolite hornfels near Hetta Lake					
7	DT72-60A (73102)	Actinolite hornfels	Actinolite	0.300,0.310, 0.310,0.312 $\bar{x}$=0.308	0.2902	10.41	13.37	0.758	216±6
				Copper Mountain pluton					
8	DT72-61B (73086)	Monzonite	Hornblende	0.729,0.729 $\bar{x}$=0.729	2.1020	11.28	6.124	0.848	102±3
9	DT72-57A (73097)	Monzonite	Hornblende	0.830,0.834 $\bar{x}$=0.832	3.6282	13.03	6.199	0.894	103±3
10	DT72-56A (73082)	Granodiorite	Hornblende	0.671,0.672, 0.670,0.671 $\bar{x}$=0.671	2.1857	10.33	6.093	0.856	101±3
11	70C110 (72070)	Granodiorite	Hornblende	0.361,0.361 $\bar{x}$=0.361	1.8417	5.652	6.198	0.568	103±3
11	70C110 (72081)	Granodiorite	Biotite	9.320,9.302 $\bar{x}$=9.311	0.4671	148.8	6.325	0.887	105±3
				Pluton cutting Keete Inlet thrust					
12	DT72-59B (73083)	Granodiorite	Hornblende	1.338,1.318 $\bar{x}$=1.328	1.8662	22.74	6.779	0.916	112±3
12	DT72-59C (73081)	Granodiorite	Hornblende	0.886,0.881 $\bar{x}$=0.883	1.8532	12.25	5.489	0.890	91.6±3 $\bar{x}$=102
				Hornfels on Dell Island					
13	DT72-55A (73084)	Hornfelsed greenschist	Actinolite	0.083,0.084, 0.082 $\bar{x}$=0.083	0.6444	1.795	8.564	0.189	141±4

[1]Constants used in age calculations: $\lambda_\epsilon = 0.585 \times 10^{-10}\ yr^{-1}$; $\lambda_\beta = 4.72 \times 10^{-10}\ yr^{-1}$; $^{40}K/K_{total} = 1.19 \times 10^{-4}$ mol/mol.

[2]Ages preceded by asterisks have been increased significantly by inherited ^{40}Ar.

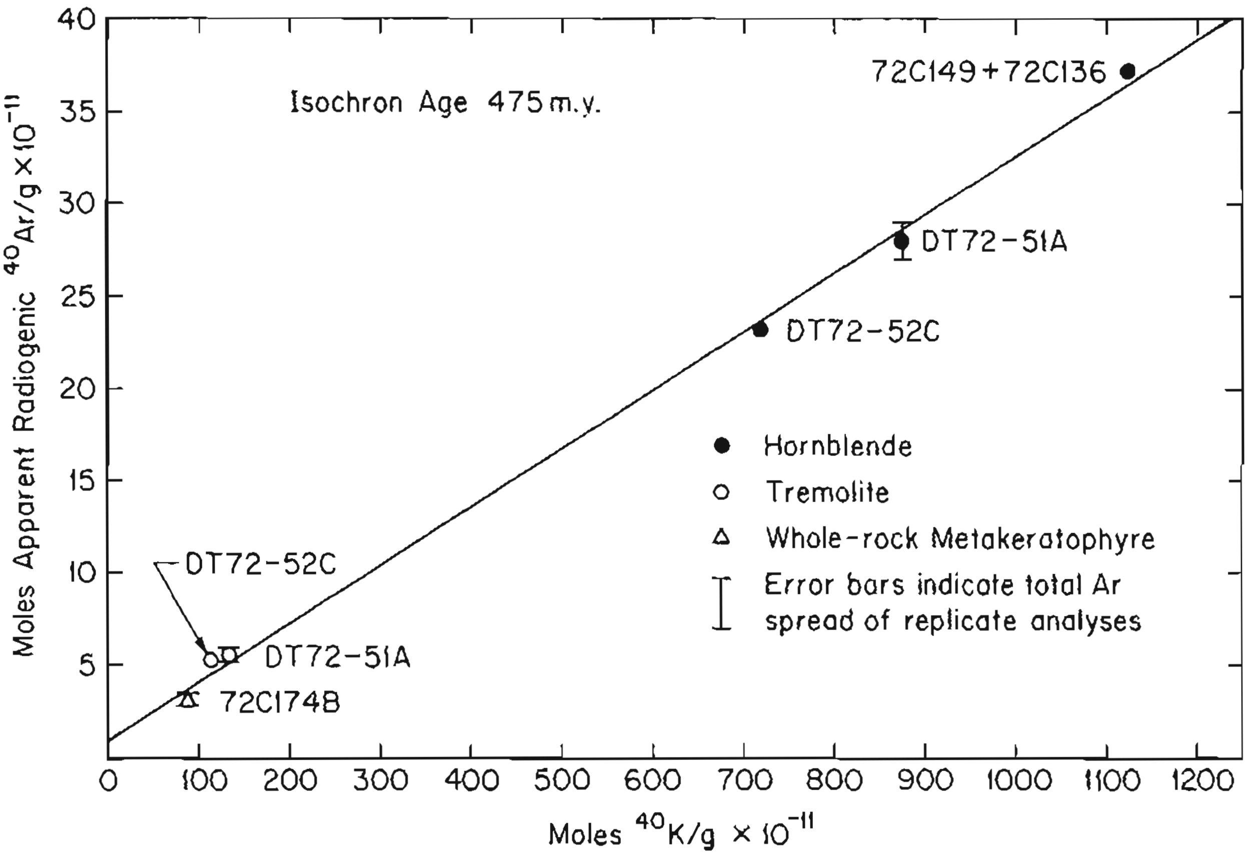

Figure 3. ^{40}K-$^{40}Ar^{rad}$ isochron for Wales Group metamorphic basement rocks.

SUMMARY AND CONCLUSIONS

Available radiometric evidence suggests that greenschist-facies metamorphism of the Wales Group occurred during Precambrian time and was followed by a regional thermal event in the Early Ordovician. Granitic and gabbroic intrusive activity occurred during the Ordovician and Silurian (about 450-420 m.y. ago). Regional thrust faulting occurred some time after the metamorphism but before the latest episode of granitic intrusive activity, which occurred in mid-Cretaceous time (102 ± 3 m.y. ago). This chronology will be of importance in the search for possible terranes to the south from which the Wales Group rocks may have been tectonically displaced.

ACKNOWLEDGMENTS

The present manuscript was reviewed by John Dillon and Wyatt Gilbert. An earlier version was reviewed by Marvin Lanphere and Michael Churkin. We are grateful to these reviewers and to Donald Eberlein for their helpful suggestions and stimulating discussions. We also wish to thank Diane Duvall, Tom Welsh, Wilfred Davis, and Kristina Ahlnas for laboratory assistance with mineral separations and K-Ar measurements. Financial assistance for the project was provided by the Alaska Division of Geological and Geophysical Surveys.

REFERENCES CITED

Brooks, A.H., 1902, Preliminary report on the Ketchikan mining district, Alaska: U.S. Geol. Survey Prof. Paper 1, 120 p.

Buddington, A.F., and Chapin, Theodore, 1929, Geology and mineral deposits of southeastern Alaska: U.S. Geol. Survey Bull. 800, 398 p.

Churkin, Michael, Jr., and Eberlein, G.D., 1977, Ancient borderland terranes of the North American Cordillera: Correlation and microplate tectonics: Geol. Soc. America Bull., v. 88, no. 5, p. 769-786.

Herreid, Gordon, Bundtzen, T.K., and Turner, D.L., Geology and mineral deposits of the Craig A-2 quadrangle and vicinity, Alaska: Alaska Div. Geol. and Geophys. Surveys Geol. Rept. 48. (In press.)

Lanphere, M.A., MacKevett, E.M., Jr., and Stern, T.W., 1964, Potassium-argon and lead-alpha ages of plutonic rocks, Bokan Mountain area, Alaska: Science, v. 145, no. 3633, p. 705-707.

Turner, D.L., Forbes, R.B., and Naeser, C.W., 1973, Radiometric ages of Kodiak Seamount and Giacomini Guyot, Gulf of Alaska: Implications for circum-Pacific tectonics; Science, v. 182, p. 579-581.

KATMAI CALDERA: GLACIER GROWTH, LAKE RISE, AND GEOTHERMAL ACTIVITY

By Roman J. Motyka[1]

INTRODUCTION

Mt. Katmai (2,047 m), located on the Alaska Peninsula in Katmai National Monument, is part of the extensive Aleutian arc system of active and sometimes violent volcanism (fig. 1). On June 6, 1912, the Katmai area was devastated by one of the largest and most dramatic eruptions in recorded history. Pumice and ash were scattered over broad regions and massive pyroclastic flows filled the valleys of Knife Creek and Lethe River, forming the famed Valley of Ten Thousand Smokes. Three days of violent eruptions culminated in the creation of the Mt. Katmai collapse caldera. The subsequent formation of a crater lake, development of intracaldera glaciers, and continuation of geothermal activity within the caldera have been documented by various investigators. The current study was undertaken to determine what changes have occurred within the caldera since Muller and Coulter's (1957) observations of 1953. Field work in August 1974 and July 1975 included resurveying the lake surface elevation, collecting water samples for geochemical analysis, taking lake-temperature measurements, and observing the growth of the lake and glaciers.

EARLY OBSERVATIONS

The 3- by 4-km Katmai caldera and crater lake were first viewed in July 1916 by Robert Griggs and his Katmai expeditionary party (Griggs, 1922). Steep, nearly vertical walls rose 600 to 1,000 m above a milky turquoise-blue lake. Large slump masses and huge rubble accumulations were present along sections of the northern and southern walls of the caldera; the rim of a volcanic cone protruded above water level near the center of the lake, evidence of postcaldera eruptive activity. The caldera was mapped and the elevation of the lake was determined in 1917 during Grigg's second Katmai excursion. Fenner and Yori visited the Katmai caldera in July 1923 (Fenner, 1930) and found the lake had drained. They descended to the caldera floor and examined the numerous mud pots, thermal springs, and fumaroles that still emanated from the relatively flat lake bed. The volcanic cone was quiescent, but a mud geyser, 30 m in diameter, was violently erupting in the northeastern part of the lake bed. Hubbard (1935) during the late 1920s and 1930s documented the refilling of the lake and the growth of permanent snow fields on the northern and southern slump masses. The lake continued to rise, attaining an elevation of 1,188 m by July 1951 (USGS topographic map, Mt. Katmai B-3, Alaska), an increase of 182 m in 28 years. By 1953 the snowfields on the slump masses had developed into glaciers, with the southern one reaching lake level (Muller and Coulter, 1957) and a third one flowing into the northwestern part of the caldera as the result of flow reversal in a glacier beheaded by the 1912 caldera collapse. By comparing aerial photographs taken in 1951 and 1953, Muller and Coulter estimated that the lake was still rising at a rate of more than 5 m per year.

RECENT OBSERVATIONS

Observations in 1974 and 1975 documented the continued growth of the glaciers and rise in lake level (fig. 2). At least 42 annual snow layers were counted in an exposed headwall of the south glacier, indicating an onset of glacier development at least by the early 1930s. All three glaciers terminate at the lake and calving occurs at several locations. The warm waters of the volcanic lake are now inhibiting any further glacier growth, and if lake level continues to rise, significant glacial ablation will probably result. However, the lake level may be stabilizing.

In August 1974 a survey of the crater lake from fixed points on the caldera rim determined the lake surface to be 1,235 m in elevation, an increase of only 47 m in the 23-year period beginning in 1951. The significantly lower rates of recent years contrast sharply with the pre-1953 rates (table 1); the increase of lake surface area with height is much too small to account for this sharp growth-rate decrease. On the basis of estimates of lake volume increases and drainage area, the 6.6-m/yr rate corresponds to 200-250 cm annual precipitation, reasonable for this coastal environment. The 2-m annual increase corresponds to an annual precipitation of 30 to 80 cm, which is low. The exact cause of the sharp decrease in lake-level rise is unknown. Perhaps at higher lake levels the pressure head is sufficient to cause considerable seepage through the Jurassic sandstones and shales of the Naknek Formation beneath the volcanic rocks. From comparison with Grigg's original map, present lake depth is estimated to be 230 m.

[1] University of Alaska Geophysical Institute, Fairbanks, AK 99701.

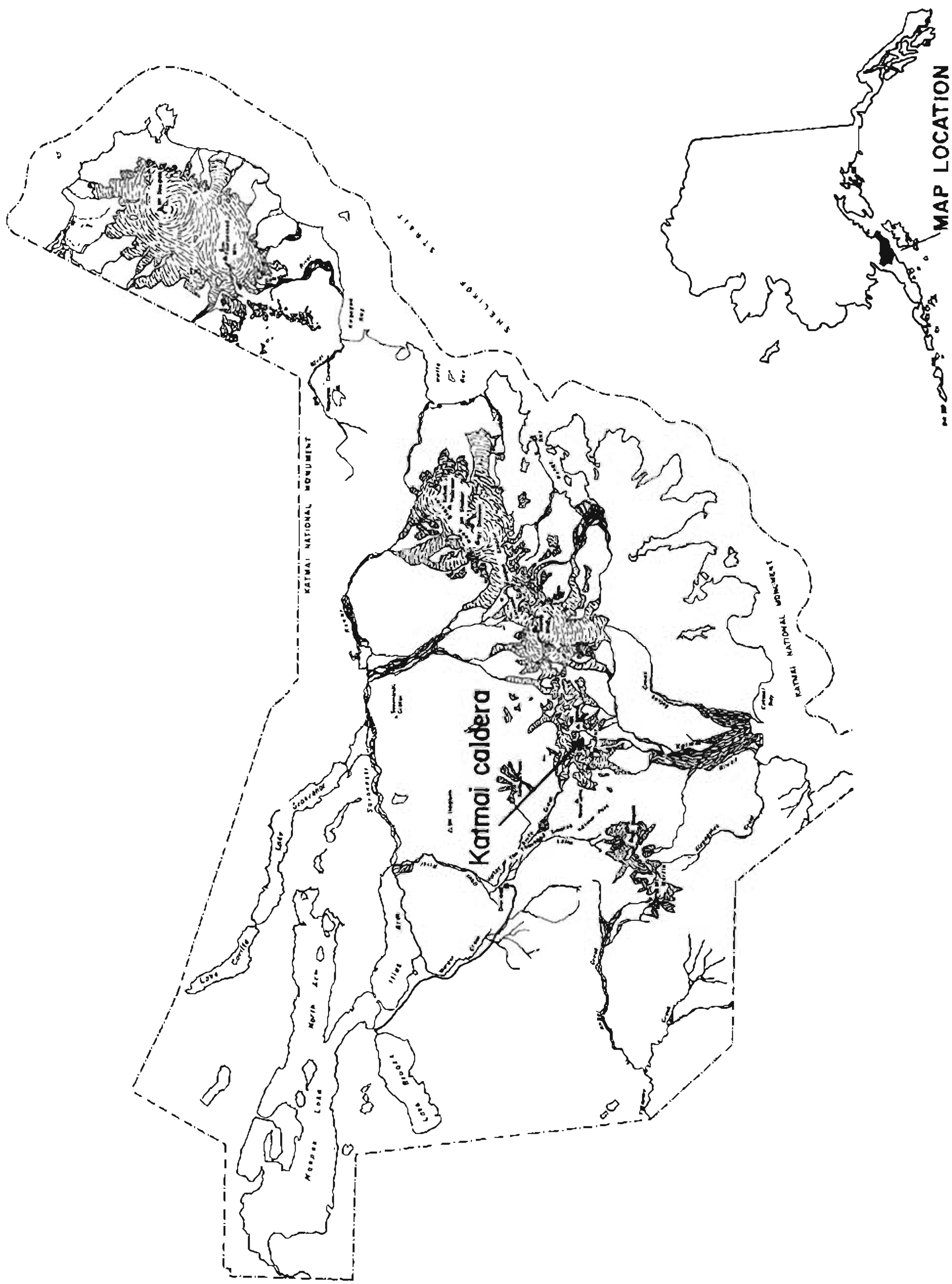

Figure 1. Location of Mt. Katmai caldera.

THERMAL REGIME, KATMAI CRATER LAKE

From interviews with local pilots who observed the lake to be unfrozen in midwinter, Muller and Coulter (1957) concluded that residual heat was still retained within the caldera. Evidence gathered in early July 1975 indicates that geothermal activity continues to affect the lake. Several stations on the lake surface were located by resectioning from several conspicuous peaks along the caldera rim. Because the inflated raft used for transportation was susceptible to wind drifting, station locations are considered rough approximations. Temperature measurements were made with a protected reversing thermometer from the surface to depths of 60 m at locations 1, 2, 3, and 5 and to 40 m at location 4 (fig. 2). The temperature profiles in four of the locations were very similar, with average temperatures of 5.3°C at 60 m and 5.8°C at 10 m (fig. 3). By using the average temperature gradient of 0.005°C/m for the 40- to 60-m depth range as representative of the entire water column, the estimated bottom temperature is about 4.5°C, which is above the temperature at which water has its highest density (4.0°C).

An estimate of the 1974-1975 crater-lake heat budget

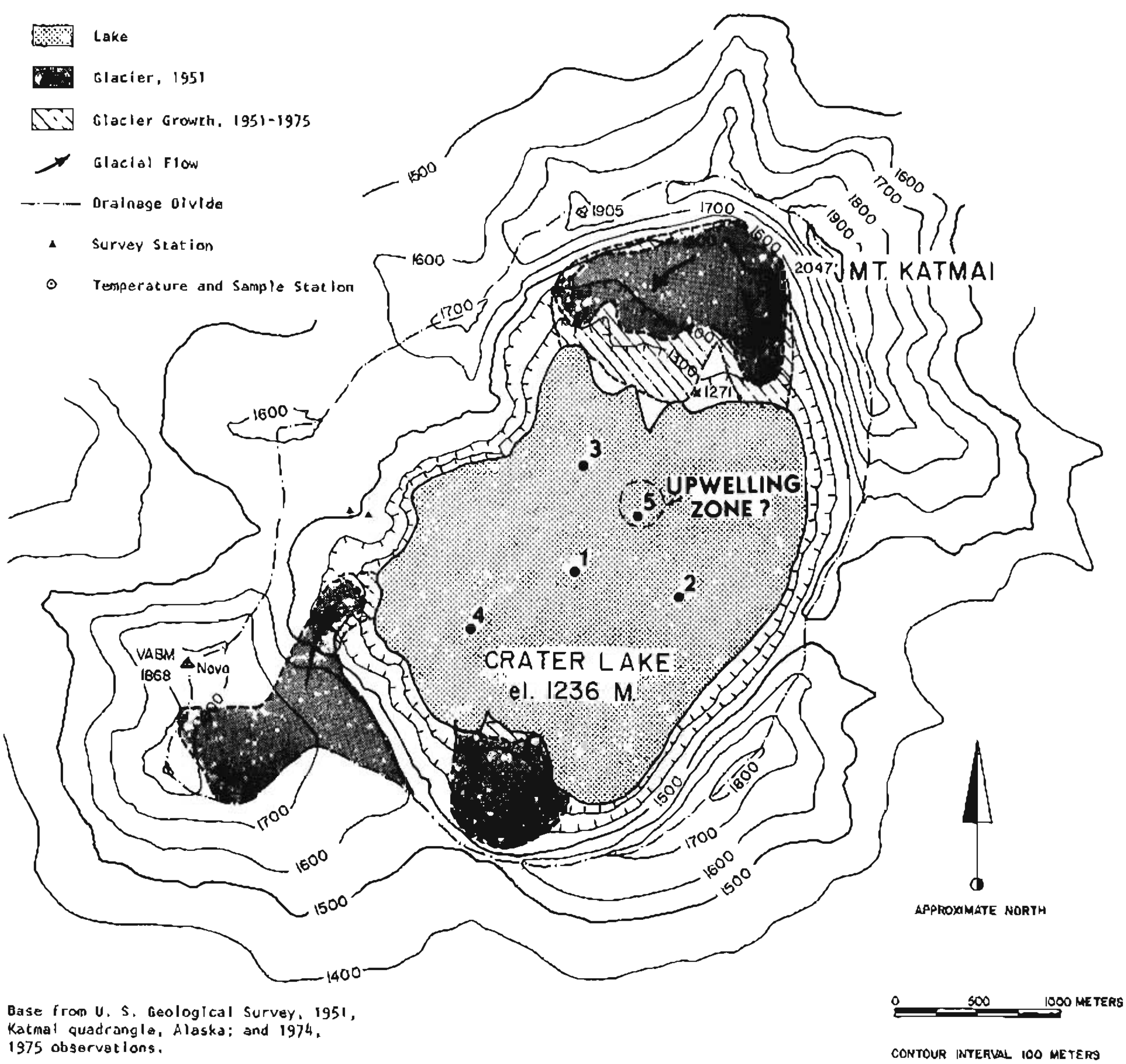

Table 1. Summary of lake level changes, Mt. Katmai crater lake

Year	Approx. lake depth (m)	Est. annual change (m)
1917	10-15	2-3
1923	0	?
1951	182	6.6
1953	- - -	5[a]
1974	229	2
1975	230	1.2[b]

[a]Estimated photo comparison (Muller and Coulter, 1957).
[b]Measured by field survey.

was made by using Michel's (1971) model for the thermal regime of deep lakes. Weather conditions at the caldera were extrapolated from weather data at King Salmon and Kodiak. A conservative lapse rate of 0.43°C/100 m was used for determining caldera air temperatures. The results of the analysis indicate that even when conservative estimates were made for all the various heat-budget factors, the July lake temperatures were still abnormally high, implying a source of heat still present at depth.

Station 5 was approximately centered over a zone of yellowish discoloration about 100 m in diameter that was easily seen from the caldera rim and which roughly coincides with the location of Fenner's "mud geyser" (1930). A temperature of 5.5°C was measured at depths of 10 and 60 m, indicating upwelling and thermal mixing. The yellowish color of this zone was caused by a dense stream of small sulfur particles that appeared to be rising from a subaqueous source. The areal extent, appearance, and location of the discoloration varied, sometimes disappearing completely for several minutes or more. This zone had a markedly different character in August 1974, appearing as a large boil of water, as if due to upwelling. The high concentrations of sulfur in this and several other areas of the lake were accompanied by continuous bubbling activity and heavy odors of hydrogen sulfide and organic gas. A pH of 2.5-3.0 was measured at all locations. Table 2 gives the geochemical analyses of water samples obtained from 60 m depth at stations 5 and 2.

Extrapolations of average temperatures from King Salmon and Kodiak indicate that the surface of the crater lake should normally freeze by early winter at the latest. The presence and growth of glaciers within the caldera also indicate a relatively cold climate. However, ERTS images taken February 11 and March 19, 1975 show the lake surface free of ice, providing further evidence of geothermal activity. However, an aerial photo taken March 14, 1967 shows the lake almost completely frozen over. The 1966-67 winter temperatures were about normal at King Salmon and Kodiak, but the 1974-75 winter temperatures were considerably below average. The lack of lake ice during an especially cold winter may indicate that Mt. Katmai is in a state of thermal fluctuation or is beginning to warm up. Significant changes in water temperatures of crater lakes preceded recent eruptions at Ruapehu Volcano, New Zealand (Dibble, 1974) and Taal Volcano in the Philippines (Minakami, 1974). Continued monitoring of Katmai crater lake appears warranted.

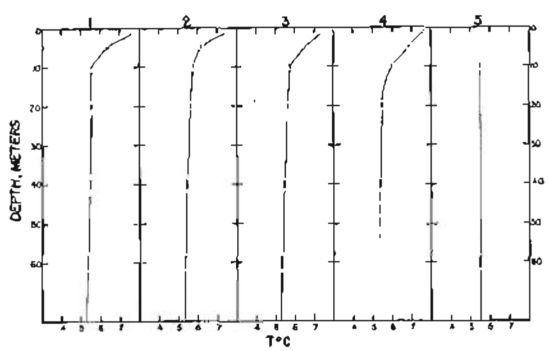

Figure 3. Temperature-depth profiles at five locations in Mt. Katmai crater lake, July 7-8, 1975. (See fig. 2 for station locations.)

Table 2. Chemical analysis of water samples from Mt. Katmai crater lake (ppm)

Location[a]	SiO_2	H	Ca	Mg	Na	K	Li	SO_4	Cl	F	B
2	120	8.9	300	51	760	90	0.92	1250	1350	0.9	12
5	140	11.4	300	62	590	110	1.2	1200	1750	1.1	14

[a]See Figure 2.

ACKNOWLEDGMENTS

Permission to conduct research in the Katmai National Monument was granted by the National Park Service. Special thanks are due to Virginia Ferrell, Steve Peterson, Axel Bachman, and Molly McCammon for their active and valuable field assistance and to Carl Benson and Richard Reger for careful review of the manuscript. Funds for the Katmai glaciers study have come from a variety of sources, including a University of Alaska Department of Geology grant, a Sigma Xi research grant in aid, the National Science Foundation, and private donations.

REFERENCES CITED

Dibble, R.R., 1974, Volcanic seismology and eruption of Ruapehu Volcano, *in* Physical volcanology (L. Ciretta and others, eds.): New York, Elsevier, p. 49-84.

Fenner, C.N., 1930, Mount Katmai and Mount Mageik: Zeitschr. Vulkanologie, v. 13, p. 124.

Griggs, R.F., 1922, The Valley of Ten Thousand Smokes: Washington, Natl. Geog. Soc., 341 p.

Hubbard, B.R., 1935, Cradle of the storms: New York, Veil-Ballou Press, 283 p.

Michel, B., 1971, Winter regimes of rivers and lakes: Cold Regions Research and Eng. Lab. (CRREL) Mon. 111-bla, 131 p.

Minakami, T., 1974, Predictions of volcanic eruptions, *in* Physical volcanology (L. Ciretta and others, eds.): New York, Elsevier, p. 313-332.

Muller, E.H., and Coulter, H.W., 1957, Incipient glacier development within Katmai Caldera, Alaska: Jour. Glaciology, v. 3, p. 13-17.

GEOLOGY AND K-AR AGE OF MINERALIZED INTRUSIVE ROCKS FROM THE CHULITNA MINING DISTRICT, CENTRAL ALASKA

By R.C. Swainbank,[1] T.E. Smith,[2] and D.L. Turner[3]

ABSTRACT

Late Cretaceous to early Tertiary K-Ar dates on micas and amphiboles from mineralized intrusives and intrusive breccias in the Chulitna mining district provide ages for endogenic metallization and associated hydrothermal alteration, which may overlie deep-seated centers of porphyry mineralization. The K-Ar ages are consistent with a post-Upper Jurassic emplacement of the ophiolite sequence in this district and support a Late Cretaceous to early Tertiary age for plate covergence at this suture zone.

GEOLOGY

The Chulitna mining district, about 30 miles long and 10 miles wide, extends northeasterly from the Eldridge Glacier along the southwest flank of the Alaska Range, about 200 miles north of Anchorage. Hawley and Clark (1973, 1974) reviewed the geology, geochemistry, and mineralization of the Upper Chulitna district and the most recent work of Jones and Silberling (pers. comm., 1977) has substantially modified the age assignments of several rock units in this district.

The structural grain of the district trends northeasterly and at least 23 pipelike(?) intrusive breccias associated with two centers of porphyritic igneous activity are present near the West Fork of the Chulitna River. Many of these breccias contain copper and silver mineralization with occasional gold and molybdenum (Hawley and Clark, 1974).

Jurassic and Cretaceous argillite, graywacke, and conglomerate along the northwest flank of the district are in conformable contact with an interlayered limestone and pillow basalt unit of Triassic age to the southeast (fig. 1). This unit is succeeded to the southeast by a sequence containing red beds, mafic volcanic rock, calcareous argillite, and limestone. Hawley and Clark (1973) suggested a Permo-Triassic(?) age for the red-bed unit. Jones (1976) assigned the unit a Late Triassic age and noted that the red beds contain blocks of older fossiliferous limestone. The most recent work of Jones and Silberling, however, indicates an age of Permian to Jurassic for this unit (pers. comm., 1977).

An ophiolite suite containing basalt, bedded chert, and serpentinized peridotite crops out along the southeast margin of the red-bed unit and is separated from it by the Upper Chulitna fault. Hawley and Clark (1973) mapped the serpentinite, gabbro, and basalt as Tertiary(?) and the bedded chert and basalt as Permo-Triassic(?), whereas Jones (1976) suggested that the chert from the dismembered ophiolite suite is pre-Tithonian (pre-Upper Jurassic). However, recent work has resulted in an Upper Devonian age assignment for this chert (Jones and Silberling, pers. comm., 1977).

Along the southeast flank of the district tightly folded Triassic(?) and Jurassic graywacke is in unconformable and partially faulted contact with the ophiolite suite to the northwest. Jones (1976) stated that this graywacke contains fossils indicative of a post-Tithonian age, and he and Csejtey (1976) indicate that the ophiolite suite of the Upper Chulitna district probably represents a post-Tithonian suture zone between Late Paleozoic and Jurassic island arc and oceanic material on the southeast side of the zone and continental material on the northwest. The age range of some of these units has been extended by the recent work of Jones and Silberling.

Hypabyssal intrusions are present throughout the district, mainly in the Jurassic and Cretaceous clastic sequence. Diorite and andesite are more common in the red-bed sequence, where they occur as plugs, dikes, and sills, and also in the Bull River area, where they apparently constitute a large part of the bedrock.

At the Golden Zone mine (figs. 1,2) a biotite quartz diorite porphyry plug is host to a breccia pipe containing copper mineralization. In the Bull River area (fig. 3), at least 22 discrete subcircular outcrops and rubble crops of breccia have been mapped. Several are highly biotitized and contain copper sulphides.

Exposures are poor in the Bull River area, but mapping of the residual(?) rubble shows that andesitic and dioritic intrusions are intruded by phaneritic granite, rhyolite, granite porphyry, rhyolite porphyry, and quartz porphyry and by a series of fine-grained aplite and felsite dikes. The granitic intrusions are themselves intruded by a coarse-grained biotite quartz monzonite porphyry and by a series of latite and basalt dikes. The breccias appear to contain fragments of all rock types except quartz monzonite and basalt and are

[1] R & M Engineering, Fairbanks, AK 99701.

[2] Solid-Earth Sciences Program, University of Alaska, Fairbanks, AK 99701.

[3] Geophysical Institute and Solid-Earth Sciences Program, University of Alaska, Fairbanks, AK 99701.

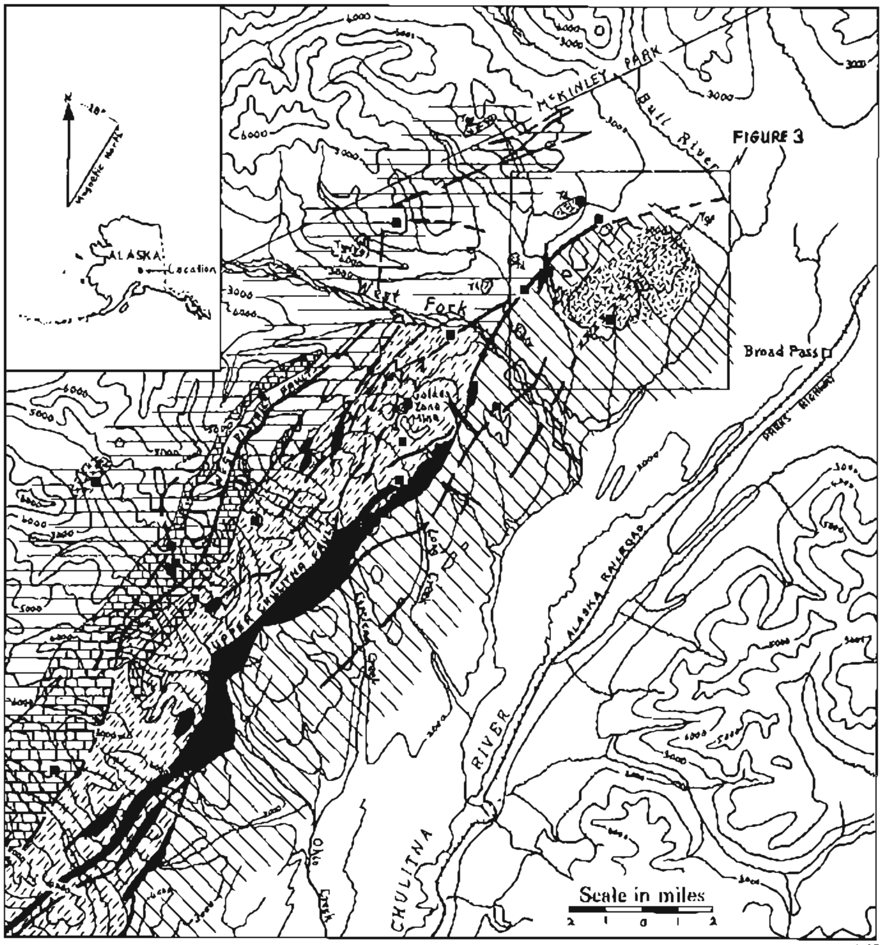

EXPLANATION

Tertiary(?) granite porphyry, quartz monzonite, aplite and quartz porphyry.

Tertiary(?) quartz diorite and diorite porphyry.

Jurassic and Cretaceous argillite, siltite, graywacke and conglomerate.*

Triassic(?) and Jurassic siliceous argillite, dark argillite and graywacke.*

Triassic interlayered limestone and basalt.*

Permian to Jurassic red beds, limestone and limy argillite.*

Upper Devonian "Chulitna Ophiolite."*

Faults and lineaments.

Lode mineral deposits and occurrences.

*Ages modified from Jones & Silberling (unpublished data).

Figure 1. Location and generalized geology (modified after Hawley and Clark, 1973).

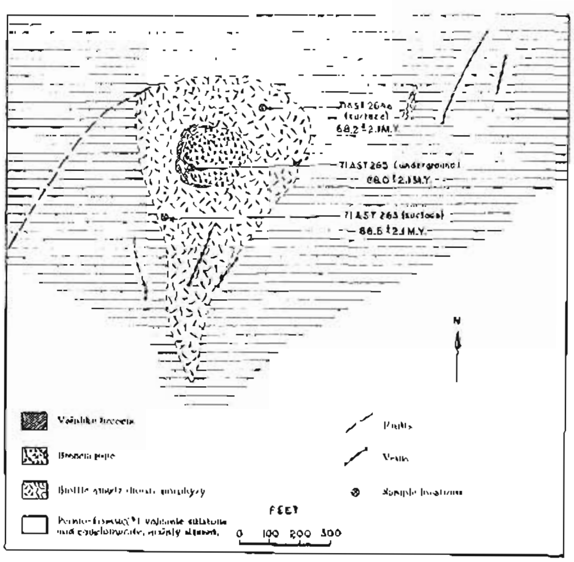

Figure 2. Generalized geologic map of the Golden Zone mine area showing locations of K-Ar age-date samples (after Hawley and Clark, 1968).

probably one of the latest phases of igneous activity. Many of the breccias in this area contain a heterogeneous mixture of angular-to-rounded fragments in a matrix of clastic material. Their emplacement appears to be controlled by preexisting faults. There is no igneous matrix and no apparent control of emplacement by igneous intrusion contacts. They fit the definition of intrusive breccias proposed by Bryant (1968).

MINERALIZATION AND ALTERATION

Production records from the Golden Zone mine indicate ore grades of 1.4 percent copper, 0.99 ounces of gold per ton, and 4.5 ounces of silver per ton. This mineralization is mostly in the periphery of the breccia pipe and is associated with intense sericitization of the host biotite quartz diorite porphyry.

Most of the mineral deposits of the district (fig. 1) are of the epigenetic vein or vein-disseminate type, and metals commonly present include arsenic, silver, copper, and gold (Hawley and Clark, 1973). Lead, zinc, bismuth, tungsten, and tin are fairly common and molybdenum is present at Long Creek, where it is associated with quartz porphyry dikes, and also in the Bull River area, where it is associated with the alkalic intrusive complex.

Selective sampling in the Bull River area disclosed a variety of copper sulphides, molybdenite, arsenopyrite, and pyrrhotite, and assays showed significant contents of gold and silver associated with the copper mineralization. Many of the intrusive breccia occurrences in the Bull River area are mineralized and are centers of potassic alteration, sequentially surrounded by sericitic, argillic, and propylitic alteration zones. The hornfels shown on figure 3 is highly siliceous and may have resulted from regional silicification.

RADIOMETRIC DATING

Samples for age determination were selected to investigate the age of alteration associated with mineralization, relative to the age of the various phaneritic igneous rocks that might be genetically associated with the mineralization. The locations of the rocks selected for age determination are shown in figures 2 and 3. Analytical data are given in table 1. Analytical work was done in the Geochronology Laboratory of the Geophysical Institute, University of Alaska, Fairbanks. Analytical techniques used have been described previously (Turner and others, 1973).

The freshest rock dated in the Bull River area, a biotite quartz monzonite porphyry, yields a biotite age of 67.0 ± 2.0 m.y. (76DS1). This age agrees well with the dates from the host biotite quartz diorite porphyry at the Golden Zone mine (68.2 ± 2.1 m.y. and 68.5 ± 2.1 m.y. for samples 71AST264A and 71AST263, respectively) and suggests that the porphyries in these two areas either were contemporaneous or had their ages reset by the same mineralizing event in latest Cretaceous time.

The age from the mineralized breccia pipe at the Golden Zone mine (68.0 ± 2 m.y., 71AST265) shows that the age of the alteration and mineralization at that locality is either coeval with the enclosing biotite quartz diorite stock or that all dated samples represent hydrothermal age overprinting of the stock. The authors favor the latter interpretation because the primary(?) biotite of sample 71AST264A is strongly chloritized and because argillic alteration is evident in sample 71AST263.

Ages from the hornblende diorite porphyry in the Bull River area (76DS3.1 and 76DS3.2, dated at 57.4 ± 1.7 m.y. and 61.2 ± 1.8 m.y., respectively) must be considered minimum ages because the dated hornblende has been substantially altered to chlorite and epidote. The age of the biotitic alteration from a mineralized intrusive breccia in this area (76DS2, 62.4 ± 1.8 m.y.) agrees within two standard deviations with the biotite age of the nearby quartz monzonite porphyry (76DS1, 67.0 ± 2.0 m.y.). The biotite in this porphyry is slightly chloritized, suggesting the presence of an age overprint, as discussed above for the Golden Zone mine.

DISCUSSION

We suggest that the mineralized breccias may indicate the presence of concealed porphyry copper-molybdenum-gold-silver mineralization, and the presence of hypabyssal calc-alkaline intrusions associated with similar mineral parageneses elsewhere in the district may

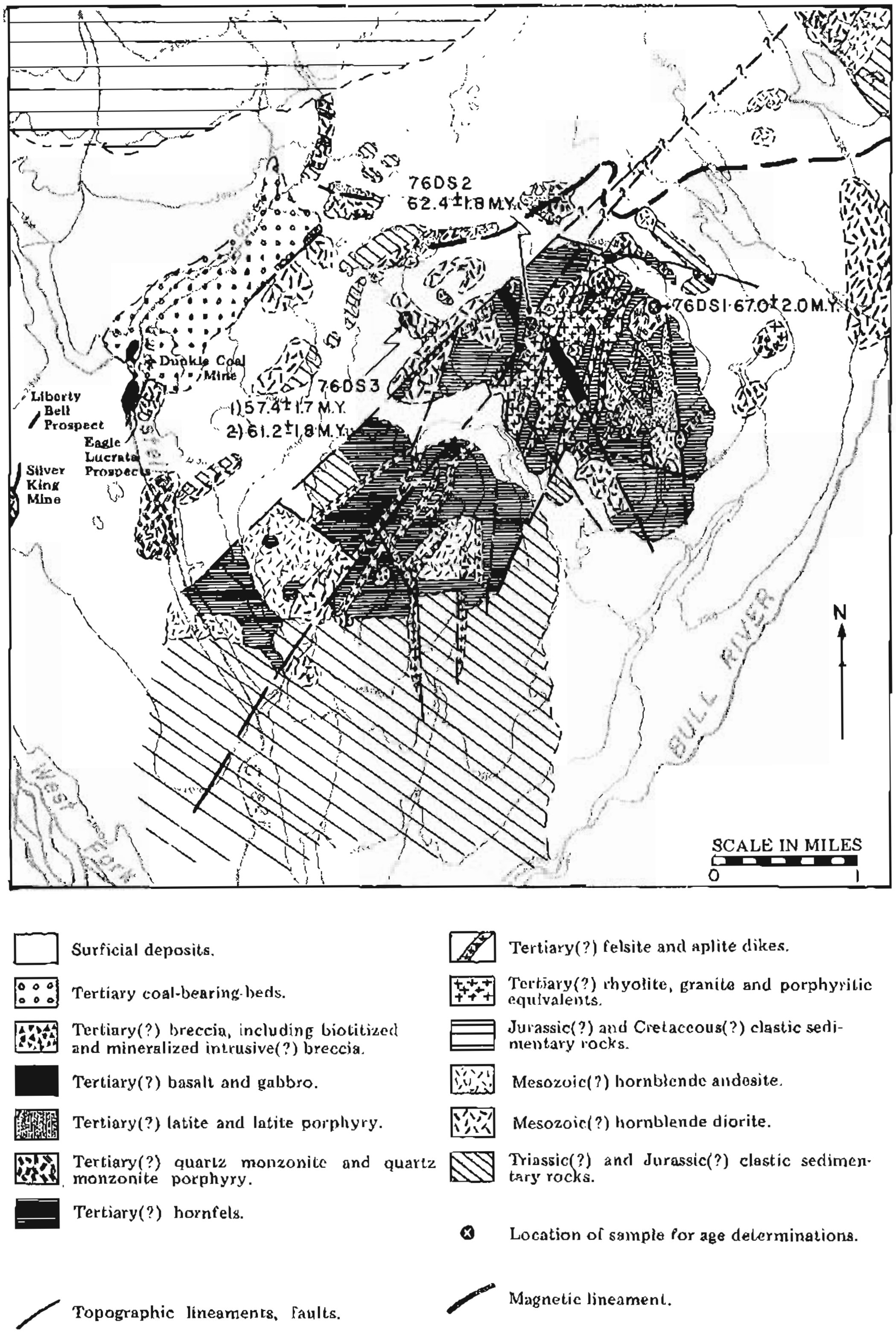

Figure 3. Generalized geologic map of the Costello Creek—Bull River area, upper Chulitna district, showing locations of K-Ar ages. (Geology by R.C. Swainbank.)

Table 1. *Analytical data for ^{40}K-^{40}Ar age determinations*[1]

Sample	Rock type	Mineral dated	K_2O (Wt.%)	Sample weight (g)	$^{40}Ar_{rad}$ (moles/g) $\times 10^{-11}$	$\frac{^{40}Ar_{rad}}{^{40}K}$ $\times 10^{-3}$	$\frac{^{40}Ar_{rad}}{^{40}Ar \text{ total}}$	Age $\pm 1\sigma$ (m.y.)
				Golden Zone Mine				
71AST263	Biotite quartz diorite porphyry	Biotite	8.317 8.340 $\bar{x}$= 8.328	1.0545	85.83	4.080	0.940	68.5 ± 2.1
71AST264A	Biotite quartz diorite porphyry	Biotite	8.340 8.347 $\bar{x}$= 8.343	0.7198	86.44	4.101	0.837	68.2 ± 2.1
71AST265	Altered breccia pipe	Muscovite	9.362 9.357 $\bar{x}$= 9.359	0.4126	95.77	4.051	0.940	68.0 ± 2.0
				Bull River Area				
76 DS-1	Quartz monzonite	Biotite	7.073 7.240 7.050 7.030 $\bar{x}$= 7.098	0.1235	71.50	3.988	0.818	67.0 ± 2.0
76 DS-2	Intrusive breccia	Biotite	8.770 8.740 8.767 8.803 $\bar{x}$= 8.770	0.1447	82.26	3.713	0.768	62.4 ± 1.8
76 DS-3 No. 1	Hornblende diorite	Altered hornblende	2.727 2.740 2.730 2.720 $\bar{x}$= 2.729	0.2142	23.50	3.409	0.841	57.4 ± 1.7 (Minimum age)
76 DS-3 No. 2	Hornblende diorite	Altered hornblende	2.100 2.010 2.000 2.060 $\bar{x}$= 2.043	0.2513	18.78	3.640	0.764	61.2 ± 1.8 (Minimum age)

[1] Constants used in age calculations: $\lambda_\varepsilon = 0.585 \times 10^{-10}$ year^{-1}, $\lambda_\beta = 4.72 \times 10^{-10}$ year^{-1}, $^{40}K/K$ total = 1.19×10^{-4} mol/mol.

represent the uppermost parts of other porphyry systems as described by the models of Sillitoe (1973) and Lowell and Guilbert (1970). The following statement by Gilmour (1977) is particularly significant: "If the intrusive breccias contain copper and other metallic minerals, or limonite derived from the oxidization of copper and/or iron sulphides, they probably overlie a buried or concealed porphyry copper system, even if the country rocks are not exposed, or if exposed are weakly mineralized or barren." Intrusive breccias containing copper sulphides are abundantly present in the Bull River area, and a breccia pipe has been mined for copper, gold, and silver at the Golden Zone mine. These breccias are associated with porphyritic intrusions in both areas. Mineralized calc-alkaline intrusions are present in at least three other localities in the upper Chulitna district, extending as far south as the Eldridge Glacier (fig. 1), which suggests that the district may contain several concealed porphyry copper deposits.

Our K-Ar ages suggest a latest Cretaceous to earliest Tertiary age for mineralization at both the Golden Zone mine and the Bull River area. The age of the spatially associated quartz diorite and quartz monzonite porphyries may have been reset during mineralization, although it is possible that mineralization was coeval with postemplacement cooling of the porphyries. These ages are consistent with early Tertiary plate convergence as postulated for other endogenetic Pacific-rim mineralization (Guild, 1972; Sillitoe, 1973). Our data suggest further age constraints on plate convergence and on emplacement of the Chulitna ophiolite, until now considered as a post-Upper Jurassic, probably Cretaceous, suture zone (Csejtey, 1976).

ACKNOWLEDGMENTS

Funding for the age dating was provided by the Alaska Division of Geological and Geophysical Surveys, and the liason and encouragement of T.K. Bundtzen of that agency is gratefully acknowledged. We thank Diane Duvall for laboratory assistance with mineral separations and K-Ar measurements. The assistance of C.C. Hawley with logistics and in collecting the samples from the Golden Zone mine is appreciated, and the permission of Resource Exploration Consultants, Inc. to use company data is likewise acknowledged. The manuscript was reviewed by W.G. Gilbert.

REFERENCES CITED

Bryant, D.G., 1968, Intrusive breccias associated with ore, Warren (Bisbee) mining district, Arizona: Econ. geology, v. 63, no. 1, p. 1-12.

Csejtey, B., Jr., 1976, Tectonic implications of a late Paleozoic volcanic arc in the Talkeetna Mountains, south-central Alaska: Geology, v. 4, no. 1, p. 49-52.

Gilmour, P., 1977, Mineralized intrusive breccias as guides to concealed porphyry copper systems: Econ. Geology, v. 72, no. 3, p. 290-303.

Guild, P.W., 1972, Metallogeny and the new global tectonics: Internat. Geol. Congress, 24th session, v. 4, p. 17-24.

Hawley, C.C., and Clark, A.L., 1968, Occurrences of gold and other metals in the Upper Chulitna district, Alaska: U.S. Geol. Survey Circ. 564, 21 p.

_____, 1973, Geology and mineral deposits of the Chulitna-Yentna mineral belt, Alaska: U.S. Geol. Survey Prof. Paper 758-A, p. A1-A10.

_____, 1974, Geology and mineral deposits of the Upper Chulitna district, Alaska: U.S. Geol. Survey Prof. Paper 758-B, p. B1-B47.

Jones, D.L., 1976, Significance of the Upper Chulitna ophiolite for the late Mesozoic evolution of southern Alaska: Geol. Soc. America (Cordilleran Section), 72nd Ann. Mtg., p. 383-384.

Lowell, J.D., and Guilbert, J.M., 1970, Lateral and vertical alteration-mineralization zoning in porphyry ore deposits: Econ. Geology, v. 65, no. 4, p. 373-408.

Sillitoe, R.H., 1973, The tops and bottoms of porphyry copper deposits: Econ. Geology, v. 68, no. 6, p. 799-815.

Turner, D.L., Forbes, R.B., and Naeser, C.W., 1973, Radiometric ages of Kodiak Seamount and Giacomini Guyot, Gulf of Alaska: Implications for circum-Pacific tectonics: Science, v. 182, p. 579-581.

THE RICHARDSON LINEAMENT - A STRUCTURAL CONTROL FOR GOLD DEPOSITS IN THE RICHARDSON MINING DISTRICT, INTERIOR ALASKA

By T.K. Bundtzen[1] and R.D. Reger[1]

INTRODUCTION

The Richardson district, along the southern margin of the Yukon-Tanana upland (fig. 1) has been a center of gold mining since the discovery of deep gold placers on Tenderfoot Creek in 1905 (Prindle, 1913; Saunders, 1965). Total known production is about 95,000 ounces of gold and 24,000 ounces of silver (Brooks, 1922; E.N. Wolff, oral comm.). In 1976 the Alaska DGGS assessed mineral resources in the Richardson district and mapped a prominent northwest-trending photogeologic lineament system that may control mineralization.

BEDROCK GEOLOGY

The bedrock of the Richardson area is composed of metasedimentary and metaigneous rocks that have undergone greenschist-to-amphibolite facies metamorphism and have been intruded by Mesozoic plutons (Foster and others, 1973). The two most common lithologies in the area are biotite-muscovite-oligoclase-quartz schist and muscovite-biotite-pennine-albite-quartz-actinolite schist (unit ms in fig. 2). F.R. Weber (oral comm.) reports sillimanite gneiss north and east of the study area. Coarse-grained K-spar-quartz-muscovite metagranite(?) (unit mg in fig. 2) occurs near the head of Buckeye Creek adjacent to several outcrops of epidote-actinolite hornfels (unit hs in fig. 2). Saunders (1965) reported metagranitic rock in the Rosa Creek drainage. A dark-green epidote-rich hornblende gneiss (unit hg in fig. 2) is exposed in an open cut in Hinkley Gulch. Hornblende from this rock has an unusually high specific gravity ($>$ 3.3) and a high K_2O content of 1.994 percent (table 1). The chemical composition of the rock (table 2) and its mineralogy suggest that it was a schist that was metasomatised and thermally metamorphosed, perhaps during emplacement of the nearby porphyry. Hornblende from the gneiss yields a minimum age of 113 $\pm$ 3.3 and 102 $\pm$ 3.1 m.y. (table 1).

Pink- to tan-weathering sericitized porphyro-aphanitic quartz-orthoclase porphyry (unit rp in fig. 2) is exposed in Democrat Creek and Hinkley Gulch, was encountered beneath Susie Creek (churn-drill boring 2 in fig. 2), and occurs in the tailings on Tenderfoot Creek (fig. 2). Quartz and carlsbad-twinned orthoclase occur as large (1 cm) euhedral phenocrysts in an aphanitic to fine-grained quartz-sericite groundmass, but the feldspar is commonly altered or absent because of weathering. The porphyry on Democrat Creek is locally gossanized and veined with quartz, and contains disseminated sulfide psuedomorphs. It yields a minimum age of 86.9 $\pm$ 2.6 m.y. (table 1), which may date the hydrothermal alteration and mineralization.

SURFICIAL GEOLOGY

The rounded bedrock ridges and hills are blanketed with extensive wind-blown organic silt of variable thickness (fig. 2). The silt has been retransported to form valley fills that are perennially frozen and ice rich (Péwé, 1975). The organic silt is 1 to 8 m thick in the drainage of Banner Creek and overlies 4 to 5 m of fluvial sand and gravel that locally contain rich placer gold deposits.

Distinct linear features identified on aerial photographs may represent a northwest-trending fracture system (fig. 1). The major feature, herein termed the Richardson lineament, extends at least 35 km from lower Tenderfoot Creek through Democrat and Redmond Creeks to the Salcha River. Although no exposures of the linear were found, the Richardson lineament appears to control the distribution of the quartz-orthoclase porphyry and the placer gold deposits. Former production shafts, associated tailings cones, and open-pit workings are concentrated along, downslope of, and downstream from the Richardson lineament on Tenderfoot, Buckeye, and Banner Creeks, in Hinkley Gulch, and near the head of Junction Creek downstream from the point of its beheading by Democrat Creek (fig. 2).

GEOCHEMICAL RESULTS

Analyses of seven chip samples of gossan-rich quartz porphyry on Democrat Creek show anomalies in silver, lead, antimony, and uranium (fig. 2, table 3). Porphyry samples from Hinkley Gulch are slightly anomalous in lead, antimony, and uranium but not gold or silver. Lead and silver values in the porphyry are coincident and lead-bearing gold-silver ore occurs in the tailings of the early drift mines on Tenderfoot Creek (Saunders, 1965).

[1]Alaska DGGS, College, AK 99708.

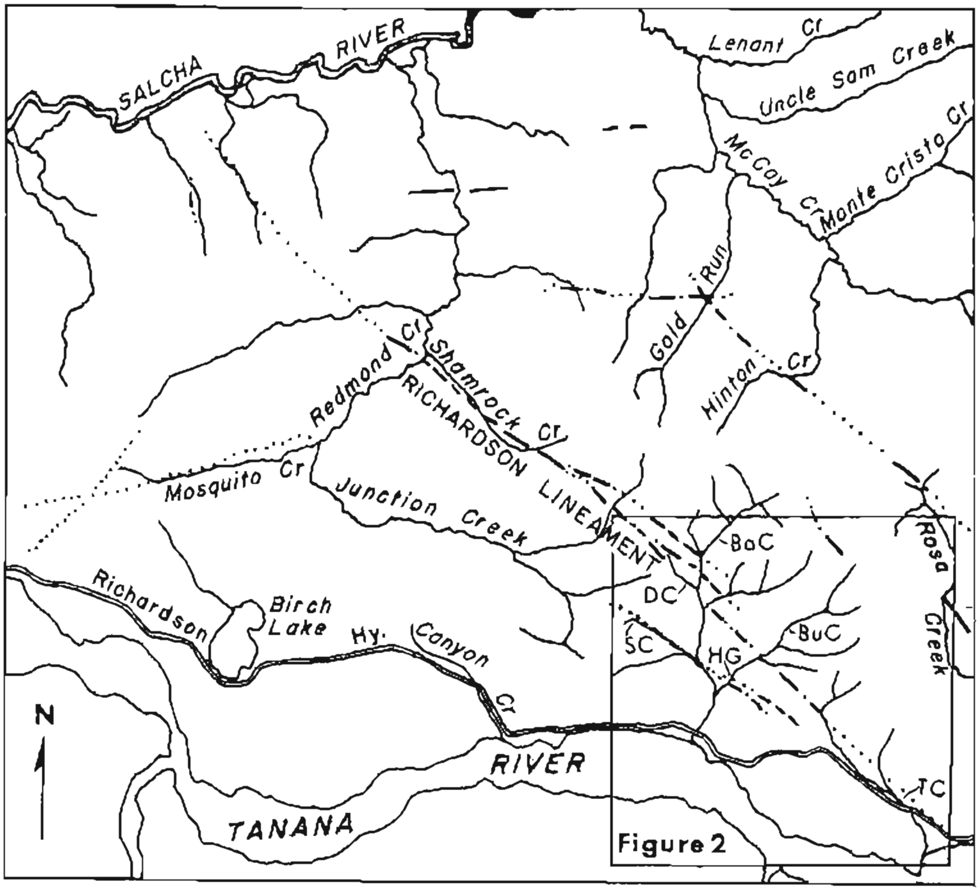

Figure 1. Major photogeologic lineaments of the Richardson mining district. Symbols: DC = Democrat Creek, SC = Susie Creek, BaC = Banner Creek, BuC = Buckeye Creek, HG = Hinkley Gulch, TC = Tenderfoot Creek. Lineaments dashed where approximate, dotted where inferred.

Gold fineness in pan concentrates from Hinkley Gulch and Tenderfoot Creek averages 670 (table 4), which is typical of the low average fineness (720) for the Richardson district reported by Smith (1941), but the samples are small and may not be representative. The low gold fineness, angularity of the placer gold, and associated base-metal mineralization led Saunders (1965) to suggest that base-metal mineralization accompanied introduction of the gold.

Pan concentrates collected during this study are rich in titanium minerals (table 4). The presence of cassiterite in Hinkley Gulch and monazite in drill-hole 4 (fig. 2) is unique, perhaps indicating a local source in the porphyry plutons. Saunders (1965) reported scheelite in pan concentrates from Democrat Creek.

CONCLUSION

In the Richardson district northwest-trending lineaments apparently control the distribution of mineralized porphyry bodies thought to be the source of placer gold. Exploration along the Richardson lineament northwest of the Banner-Democrat Creeks area may locate undiscovered placer gold and lode deposits.

ACKNOWLEDGMENTS

Special thanks are given to Gilbert Monroe, Bruce Erickson, Robert Lovelass, and Edward Smith for permission to examine their mining properties. We are also indebted to the numerous people, both cited and uncited, in particular Gilbert Monroe, who freely gave supporting data, and Wyatt Gilbert, who reviewed the manuscript.

REFERENCES CITED

Brooks, A.H., 1922, The Alaska mineral industry in 1921: U.S. Geol. Survey Bull. 739A, 47 p.

Foster, H.L., Weber, F.R., Forbes, R.B., and Brabb, E.E., 1973, Regional geology of Yukon-Tanana upland, Alaska: Am. Assoc. Petroleum Geologists Mem. 19, p. 388-395.

Péwé, T.L., 1975, Quaternary geology of Alaska: U.S. Geol. Survey Prof. Paper 835, 145 p.

Table 1. *Analytical data for K-Ar age determinations*[1]

Rock type	Sample	Mineral dated	K_2O (wt. %)	Sample weight (g)	$^{40}Ar_{rad}$ (moles/g) x 10^{-11}	$\frac{^{40}Ar_{rad}}{^{40}K}$ x 10^{-2}	$\frac{^{40}Ar_{rad}}{^{40}Ar}$ total	Age ± 1σ (m.y.)[2]
Hornblende gneiss	76BT302A	Hornblende	1.994	0.9720	34.329	6.816	0.902	113.0 ± 3.4
Hornblende gneiss	76BT302A replicate	Hornblende	1.994	0.0751	31.179	6.190	0.732	102.9 ± 3.1
K-spar quartz porphyry	76BTRich-age	K-spar	3.433	0.1127	45.121	5.203	0.881	86.9 ± 2.6

Constants used in age calculations: $\lambda_\epsilon = 0.585 \times 10^{-10}$ year^{-1}, $\lambda_\beta = 4.72 \times 10^{-10}$ year^{-1}, $^{40}K/K$ total = 1.19×10^{-4} mol/mol.

[1]Analyses performed by D.L. Turner and D. Duvall, Geophysical Institute, University of Alaska, Fairbanks, AK 99701.
[2]Minimum age.

Table 2. *Geochemical analyses of rocks from Richardson area, Alaska (wt. %)*[1]

Rock type	SiO_2	Al_2O_3	Fe_2O_3	MgO	MnO	CaO	Na_2O	K_2O	TiO_2	H_2O+	H_2O-	P_2O_5
K-spar quartz porphyry	69.3	12.6	1.9	1.0	0.03	2.0	1.1	5.8	0.38	3.0	< 0.1	0.06
Hornblende gneiss	60.3	12.5	8.3	2.0	0.20	12.0	3.5	0.63	0.60	0.1	< 0.1	0.08

[1]Done by rapid-rock technique by Skyline Laboratories, Wheatridge, CO.

Table 3. *Geochemical analyses of rock samples, Richardson district (ppm)*[1]

Map locality[2]	Sample	Au	Ag	Cu	Pb	Zn	Mo	Sb	U	Th	Sample description
1	BT 320a	0.32	7.5	58	137	21	6	150	20.5	22.5	Five chips of gossanized porphry from portal of adit above mill.
2	BT 320b	0.29	5.1	51	151	14	8	60	17.5	19.5	
3	BT 306	0.31	2.9	60	38	21	6	19	18.2	13.8	Six chips of porphyry along schist contact zone above east side of Democrat Creek.
4	BT 308	0.31	5.5	40	59	18	2	43	16.6	18.8	
5	BT 304	0.21	0.0	91	5	2	1	5	5.8	0.8	Porphyry chip.
6	BT 305	0.29	1.3	38	38	22	10	9	--	16.5	Porphyry chip.
7	BT 307	1.02	9.9	62	3,530	47	11	600	--	16.8	Porphyry chip from exposures near saddle between Junction-Democrat saddle.
8a	BT 310a	0.63	0.0	62	9	5	0	5	9.9	3.0	Amphibolite schist.
8b	BT 310b	0.33	0.0	67	17	27	6	5	9.2	1.8	Quartz-muscovite schist.
9	BT 321	0.30	0.0	45	67	52	7	9	21.9	10.3	Porphyry chip from Hinkley Gulch.
10a	BT 315	0.27	0.0	42	76	8	1	70	22.3	19.9	Eight chips of porphyry from hillside east of Hinkley Gulch.
10b	BT 319	0.31	0.0	28	40	24	6	5	14.5	24.0	
11	BT 313	0.32	0.0	47	18	20	5	5	7.4	13.0	Metagranite with pegmatitic texture.
12	BT 318	0.21	0.4	75	5	0	1	5	1.6	0.3	Chip of large quartz vein.
13	BT 302	1.33	0.0	68	17	72	1	5	--	11.5	Hornblende gneiss grab sample.

[1]Analyses by atomic absorption spectrophotometry, DGGS Minerals Laboratory.
[2]See fig. 2 for sample locations.

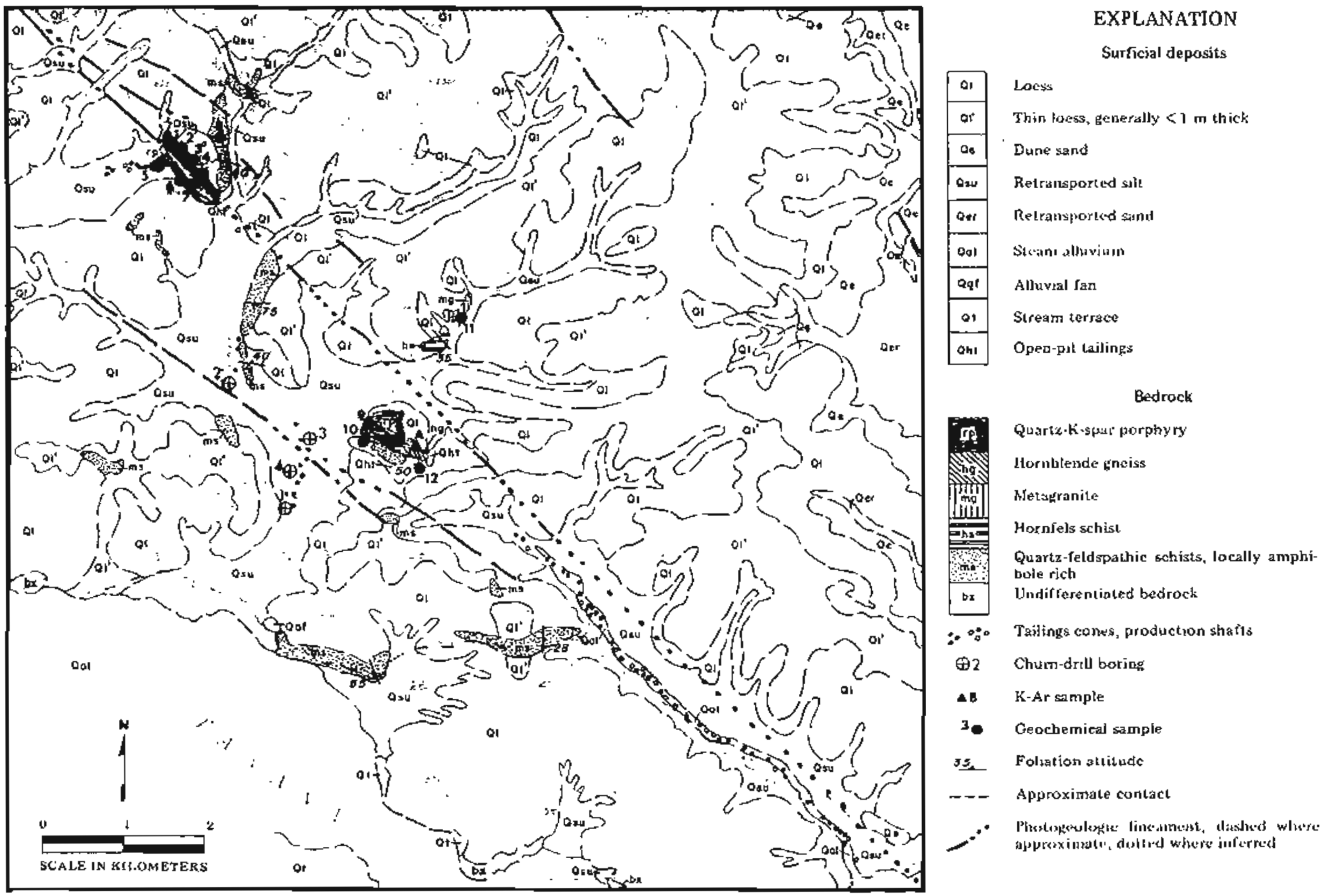

Figure 2. Geology of the Banner-Tenderfoot Creeks area, Richardson mining district, Alaska.

Table 4. *Analyses of pan concentrates from the Richardson district, 1976.*

Location	Minerals present[1] (magnetic & nonmagnetic fractions)	Gold fineness[2]	Remarks
Hinkley Gulch mine	Major: Ilmenite, rutile. Minor: Cassiterite, zircon magnetite quartz, plagioclase, epidote, garnet, gold grains - very fine and flat.	670	Based on heavy-mineral fraction obtained from mining operation in Hinkley Gulch.
Democrat Creek	Major: Garnet, ilmenite magnetite, clinopyroxene, quartz, plagioclase. Minor: Zircon, sphene. Abundant flat and angular gold.	920	Material is from three pans of 'virgin' channel deposits. Concentrate was 2% gold; also anomalous Sb (65 ppm).
Tenderfoot Creek	Major: Quartz, amphibole, clinopyroxene, garnet, magnetite, ilmenite. Minor: Zircon, sphene, gold grains - fine grained and flat.	670	From three pans of drift mine dump near first 'e' of "Tenderfoot" on fig. 2; anomalous Mo (61 ppm).
Bedrock drill-hole 2	Major: Pyrite, quartz. Minor: Dolomite, very minor gold.		Contains anomalous Cu (124 ppm), Pb (90 ppm), U (20.7 ppm).
Bedrock drill-hole 3	Major: Quartz, K-spar Minor: Magnetite, ilmenite, muscovite, very minor gold.		Contains anomalous Pb (176 ppm).
Bedrock drill-hole 4	Major: Rutile, ilmenite Minor: Monazite, scheelite, grossularite garnet, amphibole, tourmaline, zircon, fluorapatite, sphene, magnetite, epidote.		Monazite fraction (1% of concentrate) shows 280 counts/min. on DGGS scintillation counter (background is 9 counts/min).

1 X-ray work by Namok Veach, DGGS Minerals Laboratory - Major $\geq$10%; Minor $\leq$10% of sample.
2 Gold fineness by D.R. Stein, DGGS Minerals Laboratory.

Prindle, L.M., 1913, A geological reconnaissance of the Fairbanks quadrangle, Alaska: U.S. Geol. Survey Bull. 525, 220 p.

Saunders, R.H., 1965, A geochemical investigation in the Richardson area, Big Delta quadrangle, Alaska: Alaska Div. Mines and Minerals Geochem. Rept. 3, 12 p.

Smith, P.S., 1941, Fineness of gold from Alaska placers: U.S. Geol. Survey Bull. 910C, p. 147-272.

BOULDER CREEK TIN LODE DEPOSITS

By C.N. Conwell[1]

A lode-tin deposit found on Boulder Creek in the Talkeetna Mountains D-5 quadrangle (fig. 1) was explored in 1973 and 1974 by diamond drilling.

GEOLOGIC SETTING

Tin mineralization occurs within sedimentary rocks that have been subjected to both regional and hydrothermal alteration. The mineralized zone (fig. 2) lies 560 feet north of a small granite pluton (Conwell, 1973) that appears similar to the granites that are associated with the major tin deposits of the world. The deposit has been tentatively described as pneumatolytic-hydrothermal (nomenclature by Sainsbury, 1969). Although the tin mineralization is very poorly exposed, a bulldozer laid bare an area mapped by B.L. Reed of the U.S. Geological Survey and Fred McGarry of the Grandview Exploration Company as a breccia zone (figs. 2 and 3). The only recognized tin mineral is cassiterite, which varies from nearly transparent to dark brown in hand specimen.

Geochemical tin anomalies on the north flank of the Alaska Range have been reported by Reed and Elliott (1968) on Camp Creek, in the drainage immediately west of Basin Creek, and to the southeast in the drainage of Ripsnorter Creek. Tin occurs in the Yentna placers near similar granite plutons (Hawley and Clark, 1973) south of the Alaska Range, about 60 miles from Boulder Creek.

METALLURGY

Samples were tested for mineral beneficiation. In a heavy-liquid separation (specific gravity of 3.0) of a sample that had been crushed through a set of rolls to -10 mesh, 94 percent of the tin was recovered in a sink fraction that assayed 8 percent tin. A 500-g sample ground to 70 percent passing a -150 mesh screen increased the grade of the concentrate to 10 percent tin with a 96-percent recovery.

Two shaking-table tests were conducted with 5,000-g samples. The first, with the sample reduced to 100 percent -14 mesh, gave a concentrate assaying 14 percent tin with a 79.2-percent recovery. In the second table-test (70 percent of sample passing -150 mesh), 88.6 percent of the tin was recovered and the concentrate averaged 10.38 percent. The material used for these tests averaged 1.83 percent tin. Although the grade of the tin concentrate could undoubtedly be upgraded by flotation to remove the sulfide minerals, the tests indicated that simple concentration will not produce a high-grade tin concentrate.

DIAMOND DRILLING

In the exploration program 5,237 feet of drilling was completed in 23 holes. Of these, 12 drill holes intersected zones containing more than 0.53 percent tin (table 1). These holes were geometrically analyzed to determine the shape of the ore body. The indication is that 10 of the drill holes with shows of tin are in or near a plane that strikes N. 11° E. and dips 64° east; the tin occurrences in drill holes 73-2 and 74-13 do not fit the pattern. The tin occurrence in drill hole 74-7 is close to the plane, but was not used in the average for determining zone strike and dip (fig. 3).

Analyzing drill-hole locations with projections of the strike and dip of the tin vein shows six holes to be drilled too far west. No samples were taken in drill holes 74-6 and -11, the core was poor in hole 73-4, and there was 55 feet of overburden in hole 74-13. Drill holes 73-1 and 73-3 should have intersected the vein but assayed a maximum of 0.053 percent tin. The interval between 71 and 86 feet in drill hole 74-3 was assayed with negative results. In summary, from 13 holes that should have intersected a tin-bearing vein, nine had good values (a weighted average of 2.41 percent tin for an average width of 9 feet), two holes were not assayed, and two holes were negative. One drill hole, 74-11, indicated a split, or "horse," in the vein.

The associated silver values range from negative to 9.47 oz/ton (table 2). There is no firm correlation between the silver and tin.

ORE RESERVE

At this stage of exploration, the proved reserve appears small—about 150 tons which, if sold at the mid-July 1977 market value of $5.17 per lb, would gross slightly more than $1.5 million.

The inferred reserve, 523 tons, is worth $5.4 million at the above quotation.

[1] Alaska DGGS, College, AK 99701.

SUMMARY

A pneumatolytic-hydrothermal tin-bearing vein is believed present near a granite pluton, but mineralization may be limited to the breccia zone.

A small reserve of tin has been developed by diamond drilling and a larger reserve can be inferred. The resource could be several times the reserve and additional exploration is warranted. Additional drilling and metallurgical work are needed to evaluate the Boulder Creek ore body.

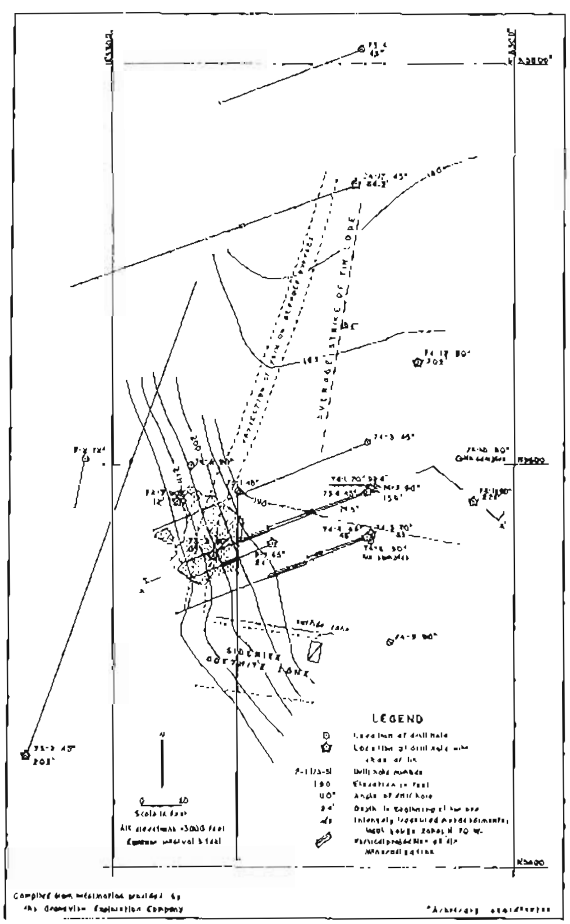

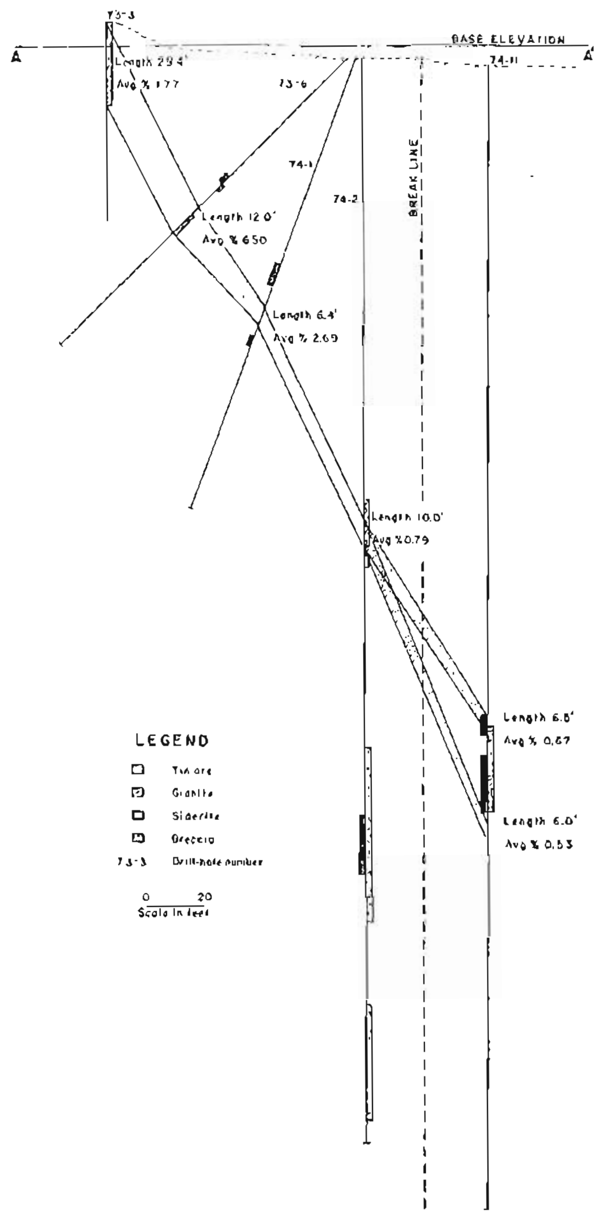

Figure 2. Drill-hole pattern.

Table 1. *Tin values from drill holes.*

Drill hole	Total depth (ft)	Angle (°)	Tin-assay depth (ft)	Length[1] (ft)	Vein width (ft)	Average assay (%)	Width x assay
P-1[2]	56.8	45	24.2	13	12.2	3.42	41.724
P-2	74.4	72	---	---	---	---	---
73-1	259.0	45	---	---	---	---	---
73-2[3]	357.2	45	220.9	0.3	---	0.62	---
73-3[2]	67.5	90	0	29.4	12.8	1.77	22.656
73-4	102.0	45	---	---	---	---	---
73-5	246.4	90	---	---	---	---	---
73-6[2]	140.0	45	74.5	12.0	11.3	6.5	73.45
74-1[2]	166.2	70	92.6	6.4	4.5	2.69	12.105
74-2[2]	377.6	90	159	10	4.4	0.79	3.476
74-3	162.6	45	---	---	---	---	---
74-4[2]	145.0	45	48	26	24.6	1.45	35.67
74-5[2]	100.7	70	83	7	4.9	0.51	2.499
74-6	239.8	90	---	---	---	---	---
74-7[3]	120.4	90	12	2	---	1.22	---
74-8	125.4	90	---	---	---	---	---
74-9	235.0	90	---	---	---	---	---
74-10	249.8	90	---	---	---	---	---
74-11[2]	395.8	90	226.2	6.5	2.8	0.67	1.876
			262.6	6	2.6	0.53	1.378
74-12[2]	273.3	90	202.0	2	0.9	0.62	0.558
74-13[3]	217.2	45	82.6	5.6	---	0.96	---
74-14	253.0	45	---	---	---	---	---
74-15	374.8	60	---	---	---	---	---
					81.0		195.392

Average width : 9.0 ft
Average assay : 2.41%

[1]Length of mineralized zone in drill hole.
[2]Used to determine strike and dip.
[3]Considered exotic occurrence.

Table 2. *Silver values from drill holes.*

Drill hole	Total depth (ft)	Angle (°)	Depth to silver (ft)	Length (ft)	Average silver (oz)
P-1	56.8	45	22.2	2	1.37
P-2	74.4	72	124.4	4.5	1.23
73-1	259.0	45	---	---	---
73-2	357.2	45	---	---	---
73-3	67.5	90	---	---	---
73-4	102.0	45	---	---	---
73-5	246.4	90	---	---	---
73-6	140.0	45	62	3	5.05
			80.5	2	
74-1	166.2	70	---	---	---
74-2	377.6	90	---	---	---
74-3	162.6	45	---	---	---
74-4[1]	145.0	45	48	4	1.40
74-5	100.7	70	---	---	---
74-6	239.8	90	---	---	---
74-7	120.4	90	---	---	---
74-8	125.4	90	---	---	---
74-9	235.0	90	35	34	3.19
74-10	249.8	90	---	---	---

Table 2. (continued)

Drill hole	Total depth (ft)	Angle (°)	Depth to silver (ft)	Length (ft)	Average silver (oz)
74-11[1]	395.8	90	67.7	196.9	9.47
74-12	273.3	90	182.4	2.1	1.11
74-13	217.2	45	82.6	3.7	1.59
74-14	253.0	45	...	...	...
74-15	374.8	60	219.1	9.3	3.24

[1]Corresponds with show of tin.

ACKNOWLEDGMENT

Appreciation is extended to the Grandview Exploration Company for allowing access to their logs and to D.L. Maynard of DGGS for performing the cartography.

REFERENCES CITED

Conwell, C.N., 1973, Grandview Exploration Company tin and silver prospects, Talkeetna (D-5) quadrangle, Alaska: Alaska Div. Geol. and Geophys. Surveys Prospect Exam. 75-4, 26 p.

Hawley, C.C., and Clark, A.J., 1973, Geology and mineral deposits of the Chulitna-Yentna mineral belt, Alaska: U.S. Geol. Survey Prof. Paper 758-A, p. A7.

Reed, B.L., and Elliott, L.E., 1968, Results of stream sediment sampling in parts of the southern Alaska Range: U.S. Geol. Survey Open-File Rept. 310, 9 p.

Sainsbury, C.L., 1969, Tin resources of the world: U.S. Geol. Survey Bull. 1301, 55 p.

COMPARISON OF MERCURY-ANTIMONY-TUNGSTEN MINERALIZATION OF ALASKA WITH STRATA-BOUND CINNABAR-STIBNITE-SCHEELITE DEPOSITS OF THE CIRCUM-PACIFIC AND MEDITERRANEAN REGIONS

By P.A. Metz[1]

INTRODUCTION

Mercury and antimony deposits worldwide have been traditionally classified as epigenetic vein deposits of the epithermal zone, whereas tungsten deposits have been classified as contact-metasomatic deposits of the mesothermal zone. Maucher (1976) has shown that much of the cinnabar, stibnite, and scheelite mineralization of the Circum-Pacific and the Mediterranean regions is both isogenetic and stratabound; he summarized the major characteristics of the Hg-Sb-W mineralization of these areas as follows:

1) The fundamental metal supply took place during the early Paleozoic and is genetically associated with basic volcanism.
2) The primary strata-bound Hg-Sb-W mineralization reacted differently to subsequent geotectonic and geothermal events. The strata-bound sequences have generally been metamorphosed to the greenschist facies and are accreted along earlier continental margins.
3) Peculiarities of younger deposits are a function of reactivities and mobilities of the elements and of differences in subsequent magmatic and metamorphic events which transformed, mobilized, and redeposited the ore minerals.
   a. Scheelite, the least mobile of the three elements, is limited to the primary strata-bound sequence except in cases of granitization and intrusion of magma, where the mineralization is localized in reaction skarns and quartz fissures.
   b. Stibnite may be found in the contacts between the primary sequence and younger rocks. During greenschist-facies metamorphism the mineralization is concentrated in lenses along fissures and fractures.
   c. Cinnabar has the greatest mobility and is redeposited in younger horizons with or without stibnite.
4) Mercury deposits are of Mesozoic-Cenozoic age.
5) The source of the Hg-Sb-W is volcanic activity along Cordilleran-type subduction zones.
6) The Hg-Sb-W association is Circum-Pacific, as evidenced by investigations in Korea, Tasmania, Bolivia, and California.

METAL PROVINCES

Cobb (1970a,b; 1975) has compiled comprehensive bibliographies on the mercury, antimony, and tungsten occurrences in Alaska. Clark and others (1974) have defined five metal provinces in Alaska that include one or more of these elements as a major constituent and five more that have one or more of the elements as a minor constituent (table 1).

The first six provinces listed in table 1 contain tungsten. The country rock types are greenschist-facies metasedimentary and metavolcanic rocks. The country rocks are Paleozoic or older and the intrusive rocks, which range from granodiorite to granite, are both Mesozoic and Cenozoic. At the major occurrences that are associated with intrusive rocks, scheelite is present in the intrusive complex (Byers and Sainsbury, 1956) in reaction skarns or within quartz veins filling fractures in the country rocks. Stibnite occurs within the six provinces as lenses, or 'kidneys,' within fractures and fissures in the schists. Mercury is present only as a minor element.

The Kuskokwim River province contains major mercury and antimony vein mineralization, and the Goodnews Bay province contains minor mercury vein mineralization. The associated country rocks are predominantly Mesozoic and include sedimentary and volcanic sequences. Intrusive rocks near the deposits range from dunite to rhyolite and are Mesozoic and Cenozoic in age. Tungsten mineralization is not present in either province.

The Chugach Mountains-Kodiak Island-Gulf of Alaska province contains several minor tungsten occurrences associated with gold quartz veins. The country rocks are greenschist-facies metamorphics. The parent rocks are trench deposits, including graywacke, shale, and associated mafic volcanic rocks. Tungsten is associated with Cenozoic intrusive rocks, which are mainly quartz diorite. No antimony or stibnite mineralization is present.

Major tungsten mineralization is present in the Hyder intrusive complex. The country rocks are Mesozoic, and the intrusive complex is Cenozoic. There is no mercury or antimony mineralization associated with the complex.

[1]Mineral Industry Research Laboratory, University of Alaska, Fairbanks, AK 99701.

Table 1. *Metal provinces in Alaska that include either tungsten, antimony, or mercury (after Clark, 1974).*

	Location of belt	Elemental associations Major	Elemental associations Minor	Associated country rocks	Age of country rocks	Associated intrusive rocks	Age of intrusive rocks	Associated major structural features
1.	Northwest Seward Peninsula	Sn-Au-F-Be	W	Siltite, phyllite, graywacke, quartz schist, and graphitic schist.	Paleozoic or older	Granite, quartz monzonite, and monzonite	Mesozoic	Numerous unnamed thrust faults.
2.	Central Seward Peninsula	Au	Hg-Pb-Ag-W	Do.	Do.	Do.	Do.	Do.
3.	Southern Seward Peninsula	Sn-W Au	Sb-Hg-F-Pb-Ag-Bi	Do.	Do.	Do.	Cenozoic	Do.
4.	Central Brooks Range	Au	Sb-W	Quartz-mica schist, mafic greenschist, calcareous schist quartzite, and graphitic schist.	Do.	Granite, quartz monzonite, and granodiorite	Mesozoic	Numerous unnamed thrust faults (major east-west fault at Wiseman).
5.	Yukon-Tanana uplands, including Fairbanks district	Sn-W Au-Pb-Zn	As-Cu-Sb-Ag	Quartz-mica schist, calcareous schist, graphitic schist and amphibolite.	Paleozoic or older (minor Mesozoic)	Granite to granodiorite	Mesozoic (minor Cenozoic)	Tintina, Shaw Creek, and Kaltag faults and unnamed faults along the Tatalina and Tolovana Rivers and Beaver and Hess Creeks.
6.	Fairbanks-Hot Springs district and north flank of Alaska	Sb-Au-Ag	Pb-Zn-Hg-W-As	Same as above plus argillite graywacke, phyllite, slate, and marble.	Paleozoic or older (minor Mesozoic and Cenozoic)	Granite to granodiorite, migmatitic granodiorite.	Mesozoic and Cenozoic	Tintina fault and unnamed faults along Tatalina and Tolovana Rivers and Beaver and Hess Creeks.
7.	Kuskokwim River region	Hg-Sb-Au	As	Volcanic graywacke, mudstone, sandstone, and shale.	Mesozoic (minor Paleozoic and Cenozoic)	Rhyolite, dacite, trachyte, and andesite.	Cenozoic (minor Mesozoic)	Farewell, Togiak-Tikchik and Iditarod-Nixon faults.
8.	Goodnews Bay area	Pt-Pd-Au	Hg-Ag-Cu	Siltstone, chert, and mafic volcanics.	Mesozoic and Paleozoic (minor Cenozoic)	Dunite and peridotite.	Mesozoic (minor Cenozoic)	Togiak-Tikchik fault.
9.	Chugach Mountains, Kodiak Island, and Gulf of Alaska	Au-Cu	Pb-Zn-Ag-W	Graywacke, shale, lava, tuff, agglomerate, mafic volcanics, and minor conglomerate.	Mesozoic	Quartz diorite.	Cenozoic	Border Ranges fault and unnamed faults on the south sides of Kodiak and Montague Islands.
10.	Hyder district	Mo-W-Cu-Pb-Zn-Au-Ag		Fine-grained schist, phyllite, and hornfels.	Mesozoic	Quartz monzonite, granodiorite, and quartz diorite.	Cenozoic	Unnamed northeast-trending fault.

Elemental

Except for the Hyder district, the major tungsten mineralization in Alaska is found in greenschist-facies metamorphic terranes of Paleozoic or older age. The metamorphic sequences include both metasedimentary and metavolcanic rocks. The major stibnite occurrences, which are found in the Fairbanks and Kantishna districts and the southern Seward Peninsula, are in these metamorphic rocks. Within the above terraces only minor isolated occurrences of cinnabar have been reported.

SUMMARY

There are many similarities between the Hg-Sb-W deposits of Alaska and the strata-bound cinnabar-stibnite-scheelite deposits of the Circum-Pacific and the Mediterranean regions, particularly the metal provinces of the Seward Peninsula, Brooks Range, Yukon-Tanana upland, Fairbanks-Hot Springs-north flank of the Alaska Range, and the Kuskokwim River region. However, the Goodnews Bay, Chugach Mountains-Kodiak Island-Gulf of Alaska, and the Hyder provinces do not fit well into Maucher's model, but the mercury and tungsten occurrences in the Goodnews Bay and Chugach Mountains areas, respectively, are few and small. The productive tungsten deposits in the Hyder district are significant, but may be explained as remobilizations from older metamorphosed source rocks. Alaskan occurrences of Hg-Sb-W should be investigated further within the strata-bound framework.

REFERENCES CITED

Byers, F.M., Jr., and Sainsbury, C.L., 1956, Tungsten deposits of the Hyder district, Alaska: U.S. Geol. Survey Bull. 1024-F, p. 123-140.

Clark, A.L., Berg, H.C., Cobb, E.H., Eberlein, G.D., and Miller, T.P., 1974, Metal provinces of Alaska: U.S. Geol. Survey Misc. Geol. Inv. Map I-834.

Cobb, E.H., 1970a, Mercury occurrences in Alaska: U.S. Geol. Survey Mineral Inv. Resource Map MR-54.

______, 1970b, Antimony occurrences in Alaska: U.S. Geol. Survey Mineral Inv. Resource Map MR-52.

______, 1975, Tungsten occurrences in Alaska: U.S. Geol. Survey Mineral Inv. Resource Map MR-66.

Maucher, Albert, 1976, The strata-bound cinnabar-stibnite-scheelite deposits, *in* Handbook of strata-bound and stratiform ore deposits (K.H. Wolf, ed.): New York, Elsevier, v. 7, p. 477-503.

EARTHQUAKE RECURRENCE AND LOCATION IN THE WESTERN GULF OF ALASKA

By J.T. Dillon[1]

INTRODUCTION

About 7 percent of the annual worldwide release of seismic energy occurs in the Alaska-Aleutian seismic belt, where the Pacific plate underthrusts the American plate (Sykes, 1971). In this region great earthquakes, which occur when the accumulated strain due to convergency exceeds the strength of the plate rocks, are more common than in all but 2 of the 51 seismic belts of the earth (Yegulalp and Kuo, 1974). This paper discusses the number, magnitude, and loci of earthquakes that may occur in the western Gulf of Alaska in the western part of the Alaska-Aleutian seismic belt during the next century. The principal source of data is the seismic history of the Alaska-Aleutian area as tabulated by Meyers (1976).

RECURRENCE INTERVAL CALCULATIONS

Since 1899 at least 80 earthquakes with Richter magnitudes greater than 6.0 (M 6+) have occurred in the western Gulf of Alaska (fig. 1). The recurrence interval for major earthquakes within a given area of the western gulf can be estimated from historic earthquake occurrence. Within the western gulf the 'historic' recurrence interval is assumed to be equal to the historic earthquake occurrence rate for the area, whereas the 'regional' recurrence interval is computed by multiplying the historic occurrence interval for the whole Aleutian Arc by the ratio of the length of arc in the western gulf to the entire length of the arc. Regional recurrence intervals also can be approximated from observed strain rates. However, incomplete geologic evidence from uplifted Holocene marine terraces suggests much longer recurrence intervals than those calculated from these other methods.

HISTORIC RECURRENCE

Historic seismicity is considered for two western gulf regions coincident except at their western boundary (fig. 1) and for two time intervals (1932-1974 and 1899-1974). Region A extends from the Shumagin Islands to Prince William Sound, parallel to the Alaska-Aleutian seismic belt. Region B, which encompasses the main area of aftershocks from the Alaska Good Friday Earthquake of 1964, is an area that apparently deforms as a structural unit (Kelleher, 1970; Sykes, 1971). Region B is truncated at 156°W. because other estimates of recurrence intervals for the Shumagin-Kodiak gap are available. The period 1932-1974 was chosen because the Alaska seismic recording network was improved in 1932 to record most M 6+ earthquakes. Only M 7+ earthquakes are considered for the 1899-1974 interval because the record is not complete for smaller events prior to 1932 (table 1).

The frequency and magnitude of M 6+ earthquakes that occurred in regions A and B between 1932 and 1974 are plotted in figure 2. If this period is representative of the seismic activity of the region, the figure shows the approximate number of earthquakes greater than a given magnitude that are likely to occur there during the next 42 years. For example, about 13 earthquakes of M 7+ should occur in region A during a 42-year interval (about 9 of these in region B alone). By dividing the number of events into the time interval considered, a recurrence interval of 3.2 years is obtained for earthquakes of M 7+ (table 1, fig. 2) in region A.

The ends of the occurrence lines on figure 2 are not well controlled. The low-magnitude end projects

Table 1. *Historic and regional recurrence intervals.*

Region[b]	Period	Method[c]	Recurrence interval at specific magnitude (yr)[a] M 6+	M 7+	M 8+
A	1932-1974	H	0.5	3	20
A	1899-1974	H	- -	4	25
A	1899-1974	R	- -	7	40
B	1932-1974	H	0.6	5	40
B	1899-1974	H	- -	6	40
B	1899-1974	R	- -	10	60
Shumagin Gap[d]	1920-1974	H	- -	8	35
	1899-1970	R	- -	- -	52 ± 20

[a]At highest measured magnitude.
[b]See fig. 1.
[c]H - Historic, R- Regional.
[d]Computations of Davies and others (1976).

[1]Alaska DGGS, College, AK 99708.

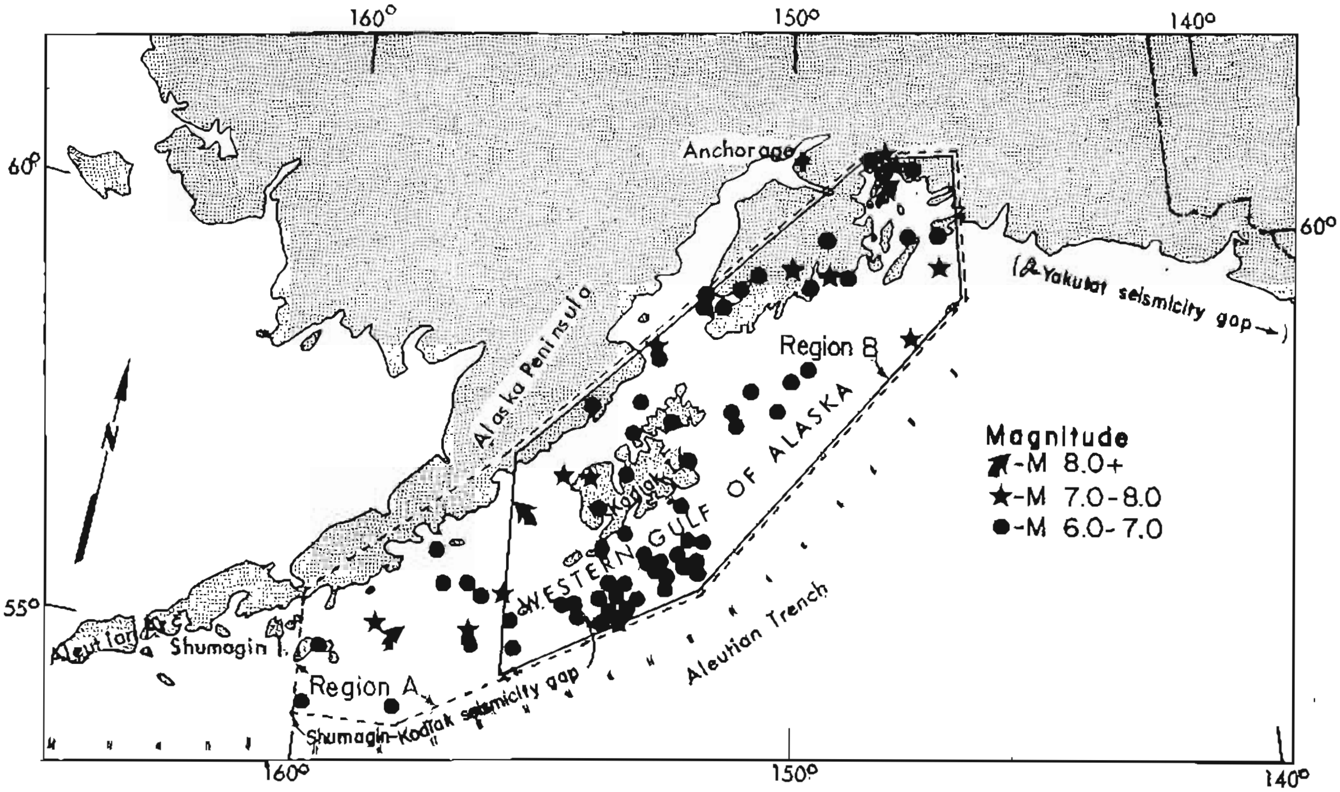

Figure 1. Earthquakes greater than magnitude 6.0 in western Gulf of Alaska, 1899-1974.

above the data points at M 6.0 and 6.25 because the network did not detect some of these earthquakes until it was improved in 1965. The 42-year time interval is barely long enough for the occurrence of a single high-magnitude (M 8+) earthquake. The data, however, suggest historic recurrence intervals of 20 years for region A and 40 years for region B for great earthquakes. Comparable historic recurrence intervals are computed for the longer 75-year seismic record (1899-1974) from regions A and B (table 1).

REGIONAL RECURRENCE

The regional recurrence interval of region A (table 1) is obtained by multiplying the historic recurrence interval of the whole Aleutian Arc - - - 2 years for M 7+ earthquakes, 10 years for M 8+ - - - by the ratio of the length of the arc in region A (1,100 km) to the total length of the arc (3,600 km).[2] This method gives a fair approximation of seismicity in the western gulf because its tectonic framework is similar to that of most of the arc. The same method was used to compute the recurrence intervals for both region B (750 km) and the Shumagin-Kodiak seismicity gap.

Sykes (1971) and Page and others (1972) show that recurrence intervals of M 8+ earthquakes derived from strain rates of converging plates are between 5 and 200 years—an interval that is too great to be of predictive use until the historic motion of the Pacific plate is better defined, but of the same order of magnitude as the intervals calculated here.

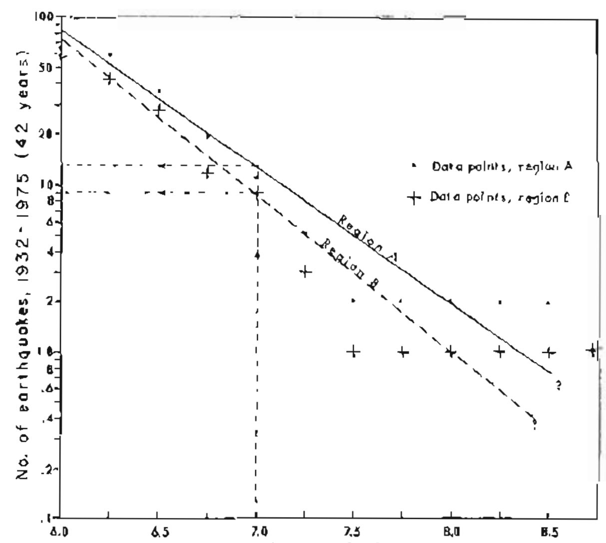

Figure 2. Earthquake frequency vs. magnitude for regions of the western Gulf of Alaska (fig. 1), 1932-74. Lines are visual averages of the occurrence rate indicated by the data points for regions A and B, respectively.

[2]See figs. 1 and 11 of Yegulalp and Kuo, 1974; and appendix II of Davies and others, 1976.

GEOLOGIC RECURRENCE

Plafker (1969) identified six uplifted marine terraces on Middleton Island that date back 4,500 years. The island was uplifted during the 1964 earthquake, and if the terraces were formed by similar seismic events, the recurrence interval for great earthquakes in Prince William Sound is 800 years, much longer than that derived by any previously discussed method. However, Sykes (1971) pointed out that terraces formed during earthquakes may not always be preserved. The average height between the terraces on Middleton Island is about 25 feet, whereas uplift during the 1964 event was 13 feet; therefore, twice as many events may have occurred and a recurrence interval of about 400 years would then be indicated. Slow regional subsidence over a long period preceded the 1964 earthquake in some of the uplifted area. This may have decreased both the net uplift and the calculated uplift intervals.

Thus, the concept of applying data from a small area such as Middleton Island to the western Gulf of Alaska is questionable. Plafker (1969) described the history of recent vertical movements in the region as "a fragmentary one based largely on rapid reconnaissance," called his conclusions "tentative," and suggested that "additional work, involving far more radiocarbon dating (of marine terraces) is required to obtain detailed data on vertical movements." Therefore, until a regional study of marine terraces in the western Gulf of Alaska becomes available, prudence dictates that the recurrence intervals of great earthquakes given in table 1 be accepted for design of earthquake and tsunamis resistent structures and other developments—especially in view of the damage wreaked by the 1964 Good Friday Earthquake (National Academy of Sciences, 1972).

EARTHQUAKE LOCATION

Large earthquakes with hypocenters in the western Gulf of Alaska will probably occur at a depth of 15-30 km along the Aleutian Benioff zone. The epicenters of M 7.9+ earthquakes can be tentatively predicted by studying the space-time seismicity pattern to discover areas that have not had major earthquakes (seismicity gaps) for unusually long times. Epicenters of future M 6 to M 7.9 earthquakes can only be predicted qualitatively.

Kelleher (1970) lists three features of space-time graphs that aid in predicting the location of large earthquakes: 1) earthquakes of M 7.9+ show strong linear trends (fig. 3a); 2) aftershock zones of successive large earthquakes are nearly adjacent but do not overlap; and 3) the direction of fracture propagation during large earthquakes is generally away from the focal zone of the previous large earthquake. This pattern suggests that the concentration of stress is transmitted systematically from one region to the next by large earthquakes and that gaps in the aftershock zones along the arc represent areas of high stored stress and high earthquake potential.

Kelleher (1970), in noting that the Shumagin-Kodiak seismicity gap was at the west end of an east-to-west progression of earthquakes and that most of the rest of the arc had ruptured since 1938, predicted that the gap will be the site of a great earthquake prior to 1980.

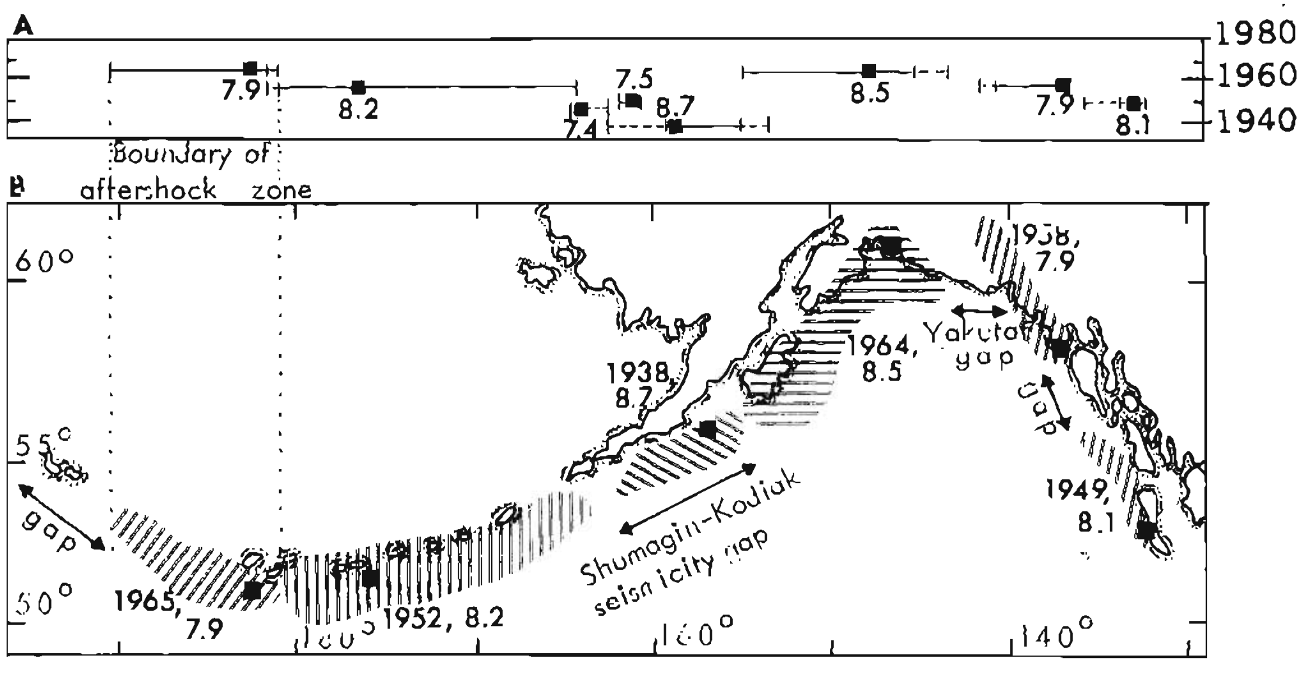

Figure 3. Space-time relationships and aftershock areas (ruled) of great Alaska earthquakes (M 7.9+) since 1930. These areas tend to abut without significantly overlapping, and probably represent rupture along major crustal blocks.

Sykes (1971), however, suggests that some of the strain in this area may have been released during two earthquakes of M 7.5 in 1946 and 1948, which diminishes the potential for a great (M 8+) earthquake before 1980. (Two M 7.5 earthquakes would release but 20 percent of the energy released by one M 8.5 earthquake.) Davies and others (1976) calculate the recurrence interval for M 8+ earthquakes in the Shumagin-Kodiak gap as 52 + 20 years (table 1). Because the last great earthquake in the gap occurred in 1938, the next one should occur in 1990 ± 20 years.

The epicenter of a great earthquake in the Shumagin-Kodiak seismicity gap should be near the south end of the Kodiak group of islands, where the aftershocks of the 1964 Good Friday Earthquake ended (fig. 4). There have been eight earthquakes of M 6.0-7.0 in this area (152-154° W., 56-57° N.) since 1965—about one per year—and the last seven M 6.0+ aftershocks of the 1964 earthquake were also located there (fig. 4).

The Yakutat seismicity gap (fig. 3) was recognized by Kelleher (1970) and Sykes (1971). Page (1975) and Page and Lahr (1976) predict that an M 8 earthquake will probably occur in the Yakutat gap within the next few decades.

The recurrence interval of great earthquakes (table 1, region A) indicates that two earthquakes of M 8+ should occur in the western Gulf of Alaska within about 60 years. One of these is likely to occur in the Shumagin-Kodiak gap and the second may occur in the aftershock region of the Good Friday Earthquake of 1964 (region B). The latter location is also consistent with recurrence-interval data for region B, which indicate that an 8+ magnitude earthquake should occur there once in every 50 ± 10 years, or between 2004 and 2024.

Magnitude 6.0 to 7.8 earthquakes are usually destructive to nearby structures, but their location cannot be specifically predicted in the western Gulf of Alaska. Seventy-five earthquakes of M 6.0 and nine earthquakes

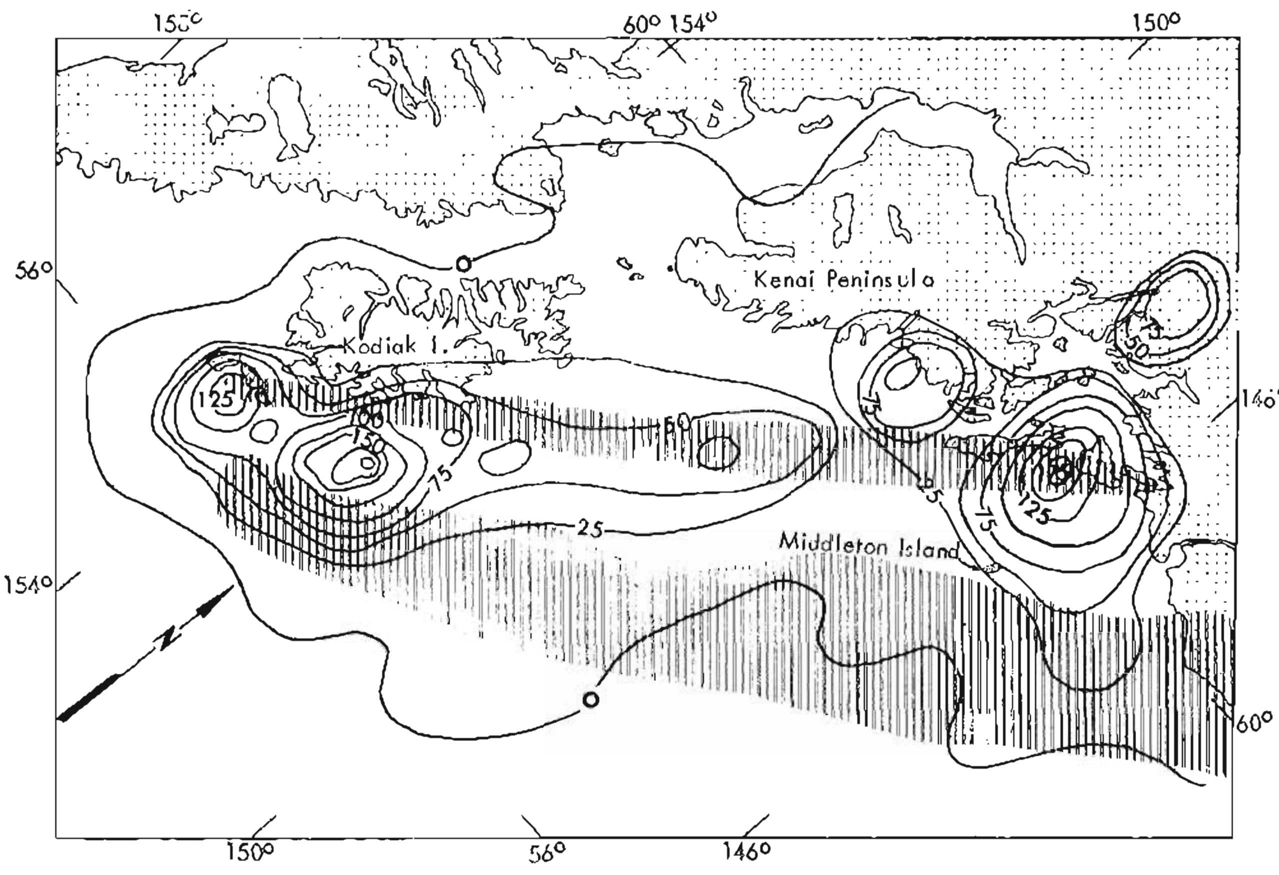

Figure 4. Strain release from the 1964 Good Friday Earthquake (contours) and deformed zones (vertically ruled) in the western Gulf of Alaska (from von Huene, Shor, and Malloy, 1972, modified with data from Bouma and Hampton, 1976). Strain-release units are 0.01 times the number of equivalent M 3.0 earthquakes per 5,200 km^2 necessary to represent the aftershocks that occurred in a unit area between 28 March and 1 May, 1964. Note the correspondence between areas of high strain release and the deformed zones.

of M 7.0+ should be expected in region B during the next 42 years (fig. 2). Many of these major earthquakes will probably occur within deformed zones (fig. 4), where there are active faults, as evinced by abundant ocean-bottom scarps (von Huene and others, 1976; USBLM, 1977, graphic 12). The location of epicenters within deformed zones is not yet predictable and should be considered random. Data from the eight recently installed seismic stations in the western gulf (Pulpan and Kienle, 1976) and microseismic data from proposed ocean-bottom seismometer networks should increase the predictability of major earthquakes.

ACKNOWLEDGMENTS

This information was initially developed and submitted to the U.S. Bureau of Land Management, Alaska OCS Office, for inclusion in the western Gulf of Alaska Draft Environmental Impact Statement. Hans Pulpan assisted in developing the methodology. I am grateful to Wyatt Gilbert and David Stone for critical review of the manuscript.

REFERENCES CITED

Bouma, A.H., and Hampton, M.A., 1976, Preliminary report on the surface and shallow subsurface geology of lower Cook Inlet and Kodiak shelf, Alaska: U.S. Geol. Surv. Open-File Rept. 76-795.

Davies, J.N., and others, 1976, A seismotectonic study of seismic and volcanic hazards in the Pribilof Islands—Eastern Aleutian Islands region of the Bering Sea, *in* Environmental assessment of the Alaskan Continental Shelf: Boulder, CO, Environmental Research Laboratories Bering Sea, Ann. Rept., v. 12, p. 1-86.

Kelleher, J.A., 1970, Space-time seismicity of the Alaska-Aleutian seismic zone: Jour. Geophys. Research, v. 75, n. 29, p. 5745-5756.

Meyers, Herbert, 1976, A historical summary of earthquake epicenters in and near Alaska: Boulder, CO, U.S. Natl. Oceanic and Atmos. Admin. Tech. Memo. Eds. NGSDC-1.

National Academy of Sciences, 1972, The Great Alaskan Earthquake of 1964, Oceanography and coastal engineering: Natl. Research Council, Natl. Acad. Sci., 556 p.

Page, R.A., 1975, Evaluation of seismicity and earthquake shaking at offshore sites, *in* Proceedings of the Offshore Technology Conference, Houston, TX, Paper 2354, v. 3, p. 179-185.

Page, R.A., and Lahr, J.C., 1976, Earthquake activity and ground shaking in and along the eastern Gulf of Alaska, *in* Environmental assessment of the Alaskan Continental Shelf: Boulder, CO, Environmental Research Laboratories Ann. Rept., v. 13, p. 69-105.

Page, R.A., and others, 1972, Ground motion values for use in the seismic design of the Trans-Alaska pipeline system: U.S. Geol. Survey Circ. 672, 23 p.

Plafker, George, 1969, Tectonics of the March 27, 1964 Alaska earthquake: U.S. Geol. Survey Prof. Paper 543-I, 74 p.

Pulpan, Hans, and Kienle, Juergen, 1976, Seismic and volcanic risk studies, western Gulf of Alaska: Fairbanks, Univ. of Alaska Geophys. Inst. OCSEAP Ann. Rept. Ru 251, 10 p.

Sykes, L.R., 1971, Aftershock zones of great earthquakes, seismicity gaps and earthquake prediction for Alaska and the Aleutians: Jour. Geophys. Research, v. 76, p. 8021-8041.

U.S. Bureau of Land Management, 1977, Western gulf-Kodiak draft environmental impact statement: Anchorage, U.S. Bur of Land Mgmt., OCS lease sale 46, 3 vol. and ref. paper 2, Physical characteristics.

von Huene, Roland, Shor, G.G., Jr., and Malloy, R.J., 1972, Offshore tectonic features in the affected region, *in* The great Alaska earthquake of 1964: Washington, DC, Natl. Acad. Sci., p. 266-289.

von Huene, Roland, and others, 1976, A summary of petroleum potential, environmental geology and the technology, time frame and infrastructure for exploration and development of the western Gulf of Alaska: U.S. Geol. Survey Open-file Rept. 76-325.

Yegulalp, T.M., and Kuo, J.T., 1974, Statistical prediction of the occurrences of maximum-magnitude earthquakes: Seis. Soc. America Bull., v. 64, n. 2, p. 393-414.